



# Viral chemistry: the chemical functionalization of viral architectures to create new technology

Zhuo Chen,<sup>†</sup> Na Li,<sup>†</sup> Shaobo Li, Madushani Dharmarwardana, Anna Schlimme and Jeremiah J Gassensmith\*

The modification of viruses using chemical conjugation techniques has brought the distant worlds of virology right into the center of nanotechnology. Viruses are naturally resilient biomolecules and this makes them exceptional templates for the creation of higher order polymers and as scaffolds for biological imaging and targeted drug delivery. In this review, we highlight progress in utilizing chemical strategies to interface viruses with synthetic polymers, to create bright bionanoparticles using synthetic fluorescent dyes, and how orthogonal chemical transformations allow for targeted drug delivery. © 2015 Wiley Periodicals, Inc.

How to cite this article:

*WIREs Nanomed Nanobiotechnol* 2016, 8:512–534. doi: 10.1002/wnan.1379

## INTRODUCTION

Viruses epitomize the structure–property relationship and superbly excel at what they do – hold delicate material, transport it through hostile environments, and deliver their payload to very specific places and under very specific circumstances. Lacking any metabolism of their own, they must either usurp the host's own machinery or they must make due with what environmental sources they can find. In short, these self-replicating, robust, and resourceful supramolecular macromolecules have evolved to become highly resilient against all manner of biological insult. This resilience has inspired, in the last decade or so, great strides in appropriating viral architecture for potential applications in energy storage,<sup>1–5</sup> energy harvesting,<sup>6–10</sup> catalysis,<sup>11,12</sup> molecular imaging agents,<sup>13–16</sup> drug delivery,<sup>17–22</sup> bio-differentiation of cells,<sup>23,24</sup> and as templates in

the preparation of both hard<sup>25,26</sup> and soft<sup>27,28</sup> materials. This interplay of cross-discipline research has created a number of incredible bio-hybrid technologies and materials.

Many viruses are adorned with protein domains for cell-recognition and payload insertion, which can be stripped from the viral genome so that researchers can produce and isolate only the nanoscopic protein shell—called the capsid—the typical location of the viral genome. Removing these components renders the viruses into noninfectious virus-like nanoparticles (VLPs), though typically they become chemically oblivious to their environment. Some native functionality can be retained and a few capsids are naturally<sup>29–31</sup> able to assemble and disassemble or change shape in response to solution pH. These natively retained features have given researchers a small number of capsids that are capable of reversibly capturing molecular cargo and releasing it, depending on local pH. Unfortunately, innate environmental responsiveness is confined to a relatively minuscule number of viral capsids and engineering this capability into new or existing capsids would be a daunting task for which very few models exist.

Viral capsids are already ideally constructed nanomaterials for medical applications as they are intrinsically capable of safely holding genomic

\*Correspondence to: gassensmith@utdallas.edu

<sup>†</sup> These authors contributed equally to this work.

Department of Chemistry and Biochemistry, The University of Texas at Dallas, Richardson, TX, USA

Conflict of interest: The authors have declared no conflicts of interest for this article.

material and transporting it in hostile environments. Harnessing that potential to act as beneficial vehicles to transport drugs and serve as nanoreactors has been an ongoing research topic in several laboratories owing to a number of advantages VLPs have over synthetic and inorganic systems. One major advantage is that viral nanoparticles can be functionalized using multiple chemically addressable surface-exposed amino acids that exist either on the wild type virus or are programmed in by site selective mutagenesis. A breakthrough example of this emerged from the Finn group in 2002 when Wang et al. described<sup>32</sup> the creation of dendritic materials from viral scaffolds. This novel contribution has since been extensively elaborated upon and is a powerful feature of VLPs. Inorganic nanoparticles, for instance, are typically monofunctional and thus placing multiple different ligands in an orthogonal fashion would be very challenging. VLPs, on the other hand, have already seen success in differential functionalization of inner and outer surfaces after successive transformations (a topic covered in this review).

Another attractive feature of viral templates is their innate monodispersity in size and volume. Synthetic nanoparticles can vary greatly in diameter and pore volume. With a precise volume, it becomes possible to load each nanoparticle with approximately the same amount of material. This precision is important, as it allows for more precise control over the stoichiometry in potential catalytic reactions, more precise control of dosage in drug delivery, etc.

Viral nanoparticles are also biodegradable, which would be an attractive feature when environmental persistence is a concern. The body's ability to filter hard materials is limited<sup>33,34</sup> to diameters less than 6 nm. Above this, the kidney can no longer effectively remove the materials and they bioaccumulate in the body's reticuloendothelial system, which prevents many nanomaterials from being clinically useful until extensive long-term toxicological analyses are conducted. This would provide VLPs a distinct advantage over non-biodegradable hard materials as protein capsids are well tolerated and, when appropriately functionalized, have clinically useful<sup>35</sup> circulatory half-lives. While it is possible that VLPs can elicit immune responses, a topic that has been recently discussed,<sup>36</sup> this is true of most recombinant drug delivery systems and, in both cases, immune passivation can be accomplished by masking the surface using, for instance, polyethylene glycol polymers.

Finally and very importantly, VLPs, while non-infectious, are still imbued with the evolutionarily endowed characteristics of the virus from which they

are descendant. These materials have been battle-hardened through evolutionary pressure to become extremely resilient against environmental threats, making them some of the most robust biomolecules in the world. Wild type viruses are also prolific replicators and can be produced typically on gram scales, even by people with fairly little exposure to biochemical techniques.

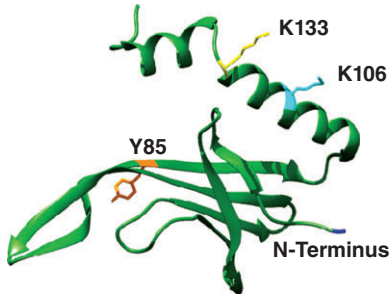

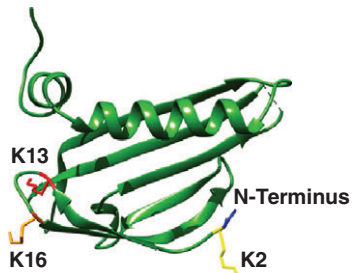
In this review, we discuss methodologies to enhance and expand these nanoscale platforms by chemically modifying the solvent-exposed amino acid residues. We will then highlight a few examples of how these chemical ligation reactions have been used to template higher order polymers, create powerful imaging agents, and operate as smart drug delivery systems.

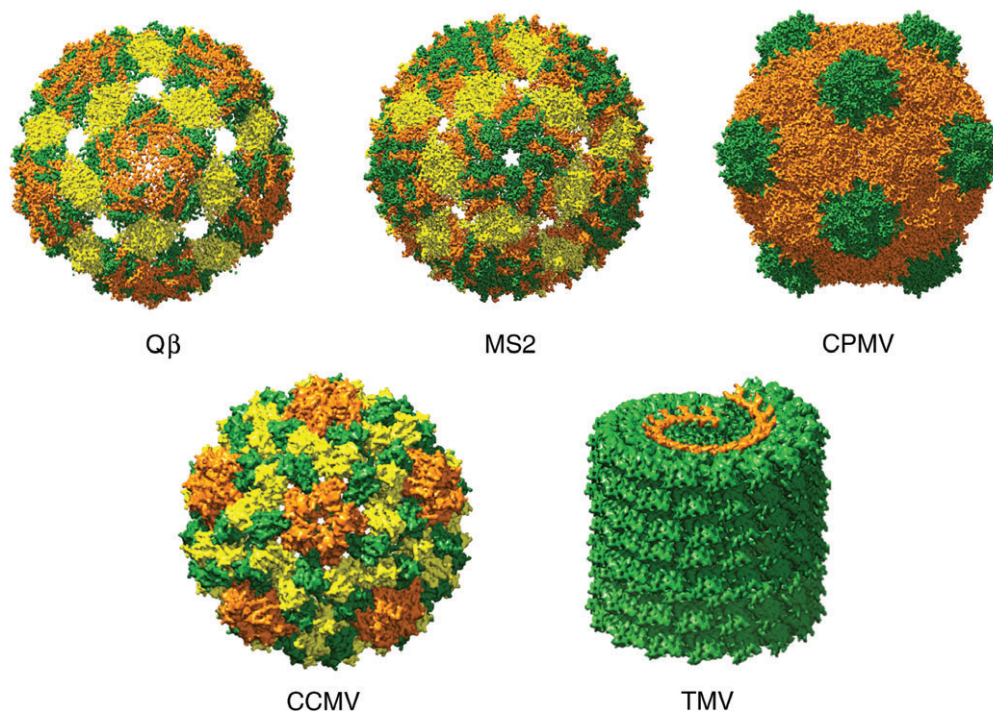
## BIOCONJUGATION

In principle, bioconjugation reactions on viruses should not differ from those on other proteins and a review on bioconjugation reactions<sup>37–39</sup> performed on viruses would be a rather truncated review on bioconjugation chemistry in general; however, viruses have some unique qualities that alter the scope of reactions and potential applications. To highlight these qualities, for the initial part of this review, we will discuss (1) the development of tyrosine bioconjugation techniques, which have largely been played out on VLPs, (2) the ability to orthogonally functionalize on different surfaces, and (3) quaternary structure in bioconjugation, which will lead in to brief overviews on polymerization, fluorescence imaging, and drug delivery with viruses. While these vignettes heavily feature three different viruses: phage Q $\beta$ , phage MS2, and tobacco mosaic virus (TMV), the reader is directed to two recent and excellent<sup>40,41</sup> reviews on filamentous phage, specifically M13. Further, Table 1 lists many functionalizations performed on these viruses, both wild type and mutant strains.

The Q $\beta$  VLP, derived from phage Q $\beta$ , a member of the *Leviviridae* family, is a 30 nm icosahedral capsid composed of 180 identical coat proteins, self assembled recombinantly within *E. coli* (though, a cell-free<sup>42</sup> synthesis has been reported). Protein crystallographic analysis<sup>43</sup> reveals (Figure 1) that the Q $\beta$  VLP possesses 20 large pores (3 nm diameter as measured atom-atom) and 12 smaller pores (1.9 nm) at the threefold and fivefold axis of symmetry respectively. These pores are sufficiently large to allow small molecules to freely diffuse between bulk solution and the interior cavity of the capsid after removal of any entrapped RNA. MS2, another

**TABLE 1** | Examples of bioconjugation reactions on MS2, Q $\beta$  and TMV.

	Residue	Reaction	Incorporated Material
	Y85	Diazonium coupling  Potassium ferricyanide-mediated oxidative coupling	diazonium salt <sup>46</sup> , FAM-SE <sup>48</sup> , [ <sup>18</sup> F]-benzaldehyde <sup>85</sup> , Gd(III)complex <sup>86</sup>  Gold NPs <sup>87</sup>
	T19pAF	NaIO <sub>4</sub> -mediated oxidative coupling  Photolysis /coupling with aniline groups	Alexa Fluor 488 <sup>88</sup> , DNA <sup>88</sup> , DNA aptamer <sup>18</sup> , fibrin <sup>89</sup> , peptide <sup>90</sup> , PEG <sup>91</sup> , porphyrin <sup>92</sup>  Live cells and DNA <sup>93</sup>
	N87C	Thiol-Maleimide	Alexa Fluor 488 <sup>18</sup> , Alexa Fluor 680 <sup>89</sup> , DOTA <sup>91</sup> , Alexa Fluor 350 <sup>92</sup> , OregonGreen 488 <sup>92</sup> , Gd(III) complex <sup>94</sup> , Taxol <sup>95</sup>
	K106, K113, N-terminus	Acylation Isothiocyanate coupling	PEG <sup>48</sup> TREN-bis-HOPO-TAM ligand <sup>86</sup>
		Y139	Diazotization and oximation <sup>47</sup> Radiolabeled by Iodogen method <sup>96</sup> Diazotization / CuAAC
E97, E106		Amide formation/ CuAAC Amide formation	Gd(DOTA) <sup>104</sup> Amines <sup>47</sup>
S123C		Thiol-Maleimide CuAAC	Maleimide derivatives of alkynes followed by azido bearing Tn antigen <sup>99</sup> , maleimide derivatives of thiol-reactive chromophores <sup>7,105</sup>
PAG (S123C mutant)		Oxidative coupling	o-aminophenols or o-catechols and potassium ferricyanide <sup>106</sup>
		K2, K13, K16, N-terminus	Acylation /click chemistry
	K2, K13 (K16M mutant)	Acylation/click chemistry	oligomannosides, <sup>60</sup> Gd(DOTA) <sup>113</sup>
	HPG	Click chemistry	oligomannosides <sup>60</sup>



**FIGURE 1** | Crystallographically obtained structures of common VLPs Q $\beta$ , MS2, Cowpea Mosaic Virus (CPMV), Cowpea Chlorotic Mottle Virus (CCMV), and Tobacco Mosaic Virus (TMV). TMV is not illustrated to scale.

member of the *Leviviridae* family, is very similar to Q $\beta$ , though slightly smaller with a 27 nm diameter. Like Q $\beta$ , MS2 possesses 32 equivalent pores and 180 identical coat proteins. A noteworthy chemical difference between the two is the presence of disulfide bonds that line the pores of Q $\beta$ , which offer a slightly higher thermal stability compared to MS2 and a solvent-exposed tyrosine in MS2, which affords a functional handle within the capsid interior.

TMV is significantly different from the above two icosahedral phage derived VLPs as it is a rod-shaped plant virus in the *Virgaviridae* family. It is much larger, being composed of 2130 identical coat proteins and self-assembles into 300 nm helical rods encapsulating the fragile genomic RNA. The external diameter of TMV is 18 nm, producing a highly anisotropic biomolecular structure. A noteworthy feature of TMV is an internal core, which has an interior diameter of 4 nm. As the oldest known virus, the structure and properties of TMV have been extensively studied over its 115+ year history.

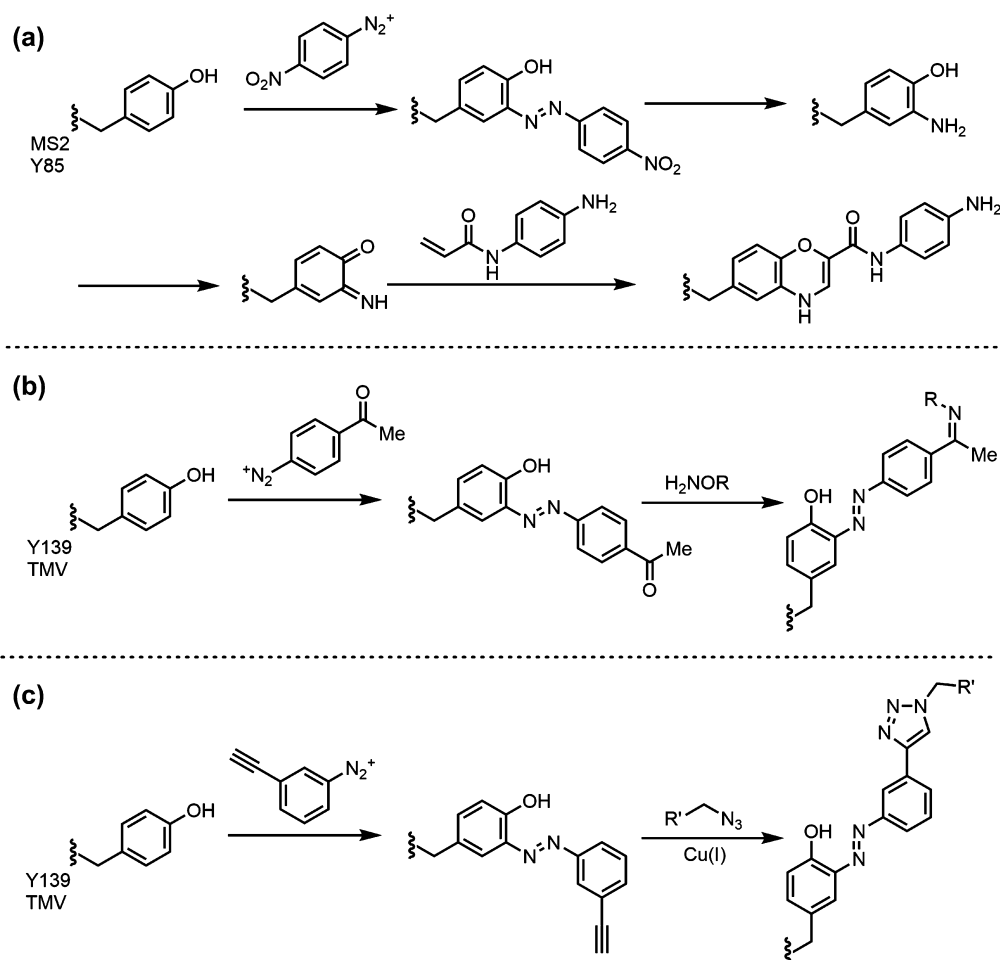
### The Rediscovery of Tyrosine Bioconjugation

Hermann Pauly, who found diazotized sulfanilic acid produced a bright red color when combined with the then-unknown amino acid histidine, first

reported<sup>44,45</sup> chemical modification of aromatic amino acids in 1904. A general lack of specificity for tyrosine over histidine and tryptophan as well as typically unfavorable reaction conditions largely sidelined the reaction until Francis and coworkers ‘reintroduced’ azo coupling on MS2<sup>46</sup> as a part of a strategy to functionalize both the interior and exterior of MS2 (*vide infra*). While the reaction was only favorable when a *p*-nitro substituted benzenediazonium salt was used, they were able to utilize it as an extensible functional handle by reducing the azo bond in the presence of sodium dithionite and subsequently re-oxidized the resulting 3-aminotyrosine to an *o*-iminoquinone derivative (Figure 2(a)). This residue could then be subjected to a hetero-Diels-Alder cycloaddition with substituted acrylamides. While the process requires several steps, it is high yielding and can be completed in a short period of time and provides a handle to future functionalization for the interior portion of MS2.

The same group then reported an improved reaction on TMV the following year, which both simplified the azo coupling as well as addressed a long-standing issue with TMV as a synthetic scaffold.

An early-articulated problem with TMV bioconjugation has been a lack of ‘canonical’ functionalizable amino acid residues exposed on the surface of



**FIGURE 2** | Azo conjugation strategies developed on VLPs. (a) The initial strategy developed by Francis and coworkers<sup>46</sup> involving hetero-Diels-Alder to place substituents. (b) Second generation Francis azo coupling<sup>47</sup> utilizing oximes to place substituents. (c) Wang azo coupling<sup>23</sup> using an alkyne-functionalized diazonium for CuAAC chemistry to place substituents.

the virus. That said, it does display a tyrosine residue on the solvent-exposed exterior surface. A noteworthy benefit of TMV over MS2 is its greater tolerance toward a broader scope of azo coupling conditions, which allowed Schlick et al. greater flexibility<sup>47</sup> in the choice of substituted benzenediazonium salt. Here, they found attachment of *p*-acetylbenzenediazonium salts gave yields in excess of 90%. As shown in Figure 2(b), the introduced ketones could then be further modified by oxime formation with impressive scope. A few years later, Wang and co-workers introduced<sup>23</sup> a strategy to allow for a more amenable CuAAC reaction (Copper(I)-catalyzed azide alkyne cycloaddition) in lieu of oxime formation by using an *o*-ethynylbenzenediazonium salt. This discovery provides two major advantages: (1) the CuAAC reaction has already been extensively studied and optimized for bioconjugation and (2) a ‘click-chemistry-economy’ for peptides, nucleotides, and fluorophores

exists in that these compounds are commercially available, which allows researchers who do not have an extensive organic or synthetic background to buy premade ‘click’ conjugates and simply attach them to the surface of the alkyne-functionalized biomolecule.

### Surface Differentiation

As hollow structures, each virus contains two discontinuous surfaces with amino acids that are only accessible from either the inside or the outside of the capsid. It is possible to chemically address both sides independently using orthogonal reaction methodologies. The first report of this being done on icosahedral viral capsids emerged from the Francis group, who found<sup>48</sup> that it is possible to orthogonally functionalize both the interior and exterior of the bacteriophage MS2 capsid. As discussed in more detail later, the group modified the exterior surface with

cell targeting DNA aptamers selectively while the interior of the capsid was modified with photoactive singlet oxygen sensitizers. Since then a lot of work has been done placing targeting ligands on the outside of a virus and hiding therapeutics inside the virus. This makes chemical sense—targeting ligands need to be outward facing toward their target while hiding the drug away inside the capsid keeps it from straying to off target sites or being prematurely deactivated. It also frees the outside surface to maximize the amount of targeting ligands without interference from adjacent drug molecules.

## POLYMERIZATION OF VLPs

In recent years, the idea of attaching or growing synthetic polymers onto or within viral protein capsids has stimulated research suggesting these virus-polymer conjugates hold promise in drug delivery,<sup>49</sup> gene-therapy,<sup>50,51</sup> and material fabrication.<sup>52</sup>

Presently, the methods to create polymer-virus conjugates are divided into two main strategies—*graft to*<sup>28,47,49,52–55</sup> and *graft from*.<sup>27,56–58</sup> The ‘graft to’ approach involves attaching long polymer chains directly to the surface, while the ‘graft from’ approach involves building a polymer up from attached initiators bound to the surface. ‘Graft to’ approaches are mostly used in polymer attachments to the outer surfaces of VLPs and, thus far, at surface-exposed lysine (CPMV, CCMV, and Q $\beta$ ) or tyrosine residues (TMV). In these cases, end-functionalized polymers can be attached directly to surface-exposed functional groups via one of a handful of the prior discussed conjugation methods.

To increase the polymer yield on the surface as well as obtain better control over the polymerization, a ‘graft from’ strategy has been employed using small-molecule initiators that can be loaded more densely on the surface. The initiators are then used in a follow up polymerization step that, in principle, forms a well-controlled, synthetic shell across the exterior surface.

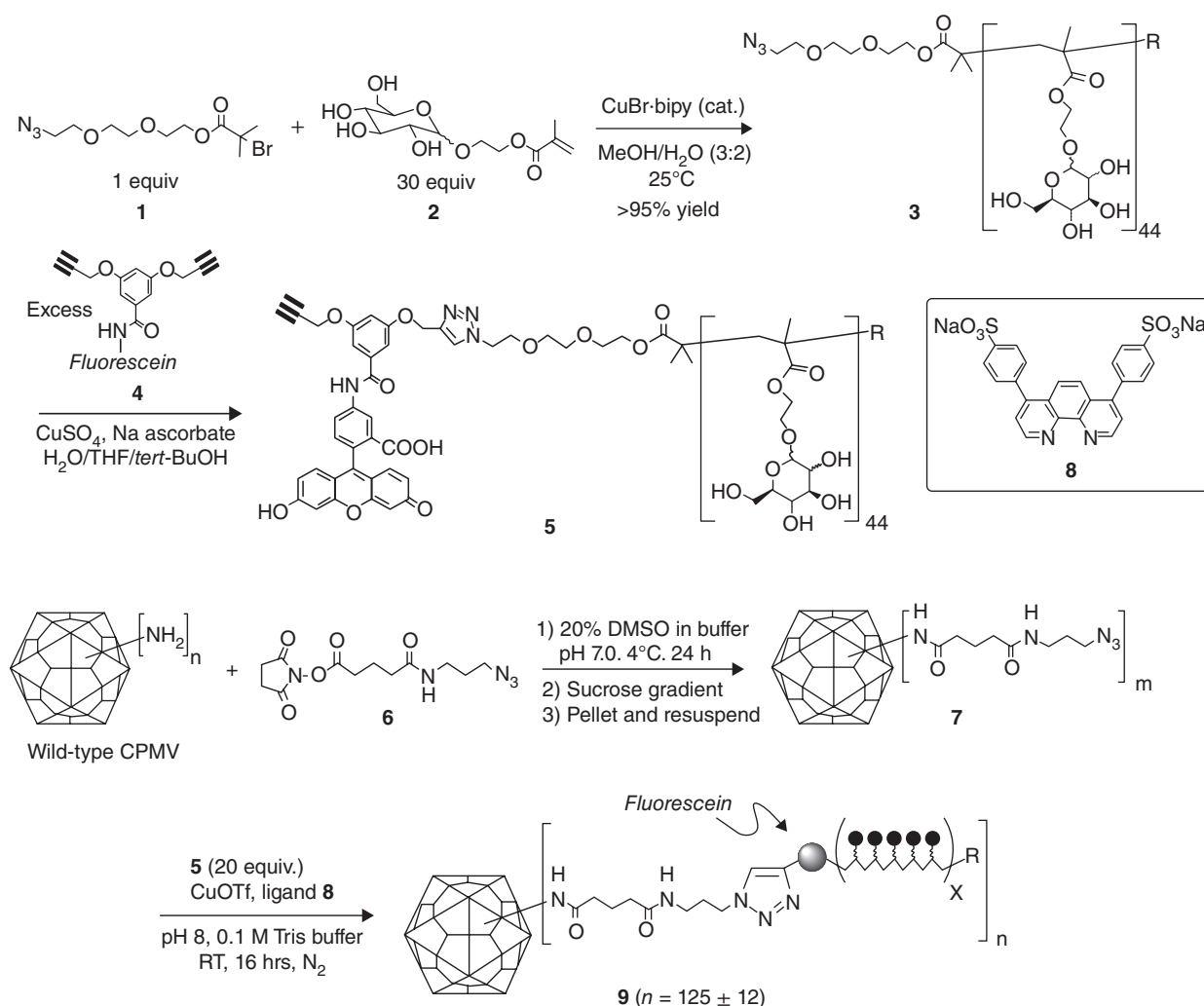
In either case, the attached polymers on the *exterior* are capable of imparting more desirable physical properties<sup>47,52</sup> and biocompatibility<sup>49–51</sup> into VLPs. For instance, improved solubility in an extended range of organic solvents, enhanced thermal stability, and reduced immunogenicity have been observed from these synthetic polymer-virus conjugates lending promise to the applications mentioned above, some of which are described in detail below. While sufficient studies on changes in physical stability have yet to occur for polymerizations within the

*interior* shell of VLPs, several pioneering reports have demonstrated great potential in loading high-density functional molecular cargo<sup>56,57</sup> and encapsulated cell binding agents.<sup>27</sup>

## ‘Graft to’ Approaches

Straightforward examples of ‘graft to’ approaches are illustrated by Finn<sup>55</sup> and Nolte<sup>53</sup> using polyethylene glycol (PEG). Finn<sup>55</sup> reported conjugating NHS ester end-functionalized PEG chains with molecular weights ranging from 2000 to 5000 to the surface-exposed lysine residues on CPMV to produce the PEGylated conjugate. The covalent attachment was confirmed using denaturing gel electrophoresis, sucrose gradient ultracentrifugation, and fast protein liquid chromatography (FPLC). The number of attachments was quantified by comparing the absorbance intensity of dye-labeled PEGs to the known concentration of capsid protein. The result revealed that PEGs with lower molecular weight (PEG-2000) obtained a much higher yield on the surface—in some cases more than one PEG per subunit. This contrasts with only about half of the reactive lysine subunits being successfully functionalized with higher molecular weight PEG (PEG-5000). Similarly, the Nolte group<sup>53</sup> grafted NHS ester-terminated PEG with a molecular weight of 3000 Da to reactive surface amine groups on CCMV. Under optimized conditions, the VLPs can yield 2–3 PEGs on each protein subunit. This higher yield compared to Finn’s work is likely a result of the relatively low molecular weight PEG they used as well as more reactive and accessible amine groups on CCMV.

Polymers have been successfully attached to the surface of VLPs using CuAAC chemistry, which has been used to improve the efficacy of ‘graft-to’ approaches. CuAAC has proven to be a robust bioconjugation strategy,<sup>59</sup> particularly under dilute conditions making it invaluable when the material to be conjugated is precious. Gupta et al.<sup>54</sup> demonstrated an alkyne-terminated neoglycopolymer can be attached to the outer shell of CPMV by CuAAC after installation of azide groups via acylation to the exterior surface lysines, as illustrated in Figure 3. The number of covalently attached polymers was determined to be  $125 \pm 12$  out of approximately 150 -azide-labeled lysines per particle, indicating an excellent yield. Recognizable changes in size and shape of polymer-virus conjugates were captured via transmission electron microscopy (TEM) and dynamic light scattering (DLS). In another publication, Manzenrieder et al.<sup>28</sup> applied this robust CuAAC strategy but with adoption of



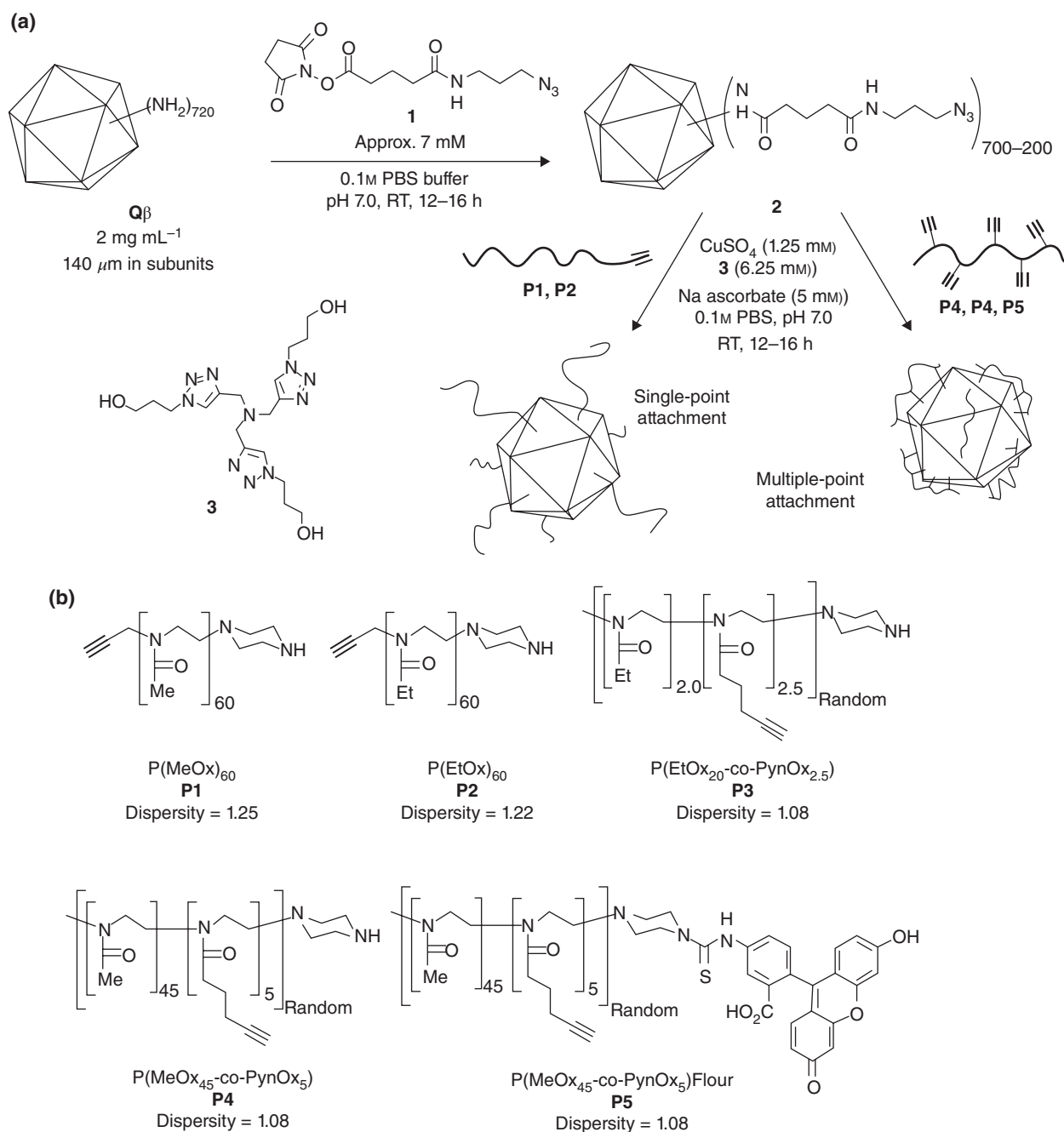
**FIGURE 3** | Scheme of ATRP of neoglycopolymer (1→3), fluorescein attached to polymer termini via alkyne-azide coupling (3→5), and fluorescein-labeled polymer attached to CPMV exterior (6→9). (Reprinted with permission from Ref 54. Copyright 2005 Royal Society of Chemistry)

poly(2-oxazoline)s containing either single (single-point) or multiple (multi-point) alkyne-functionalized side chains. Using the multi-alkyne-functionalized side chains, the group created a ‘crosslink’ of polymer and VLP from discrete covalent attachment points established on the outer shell of Q $\beta$  (Figure 4). The physical consequences of these two strategies are discussed in more detail below. Apart from functionalization on lysine groups on the icosahedral capsids, the tyrosine groups on the outer shell of TMV have served as a capable site for covalent attachment to polymer chains. Schlick et al.<sup>47</sup> illustrated a ‘graft to’ approach following the introduction of a ketone to the surface-exposed tyrosine groups by diazonium coupling. PEGylation on the exterior surface of TMV was achieved via oxime formation (*vide supra*) with alkoxyamine-derived PEG. The resultant polymer-

virus conjugates were obtained with a 50–60% coupling efficiency (out of 2130 subunits) and showed solubility in an extended range of organic solvents.

### ‘Graft from’ Approaches

The ‘graft from’ route aims to provide a more delicate manipulation of the composition and properties of attached polymers, as well as retention of the uniform size and shape of VLPs. Pokorski et al.<sup>58</sup> reported the generation of poly(oligo(ethylene glycol)-methacrylate) (poly(OEGMA)) and its azido-functionalized analog on the outer shell of Q $\beta$ . To do this, the group first constructed a Q $\beta$  ATRP macroinitiator by appending azide groups to the surface-exposed lysines. They then attached a triglyme-based ATRP initiator via CuAAC chemistry (Figure 5 compounds



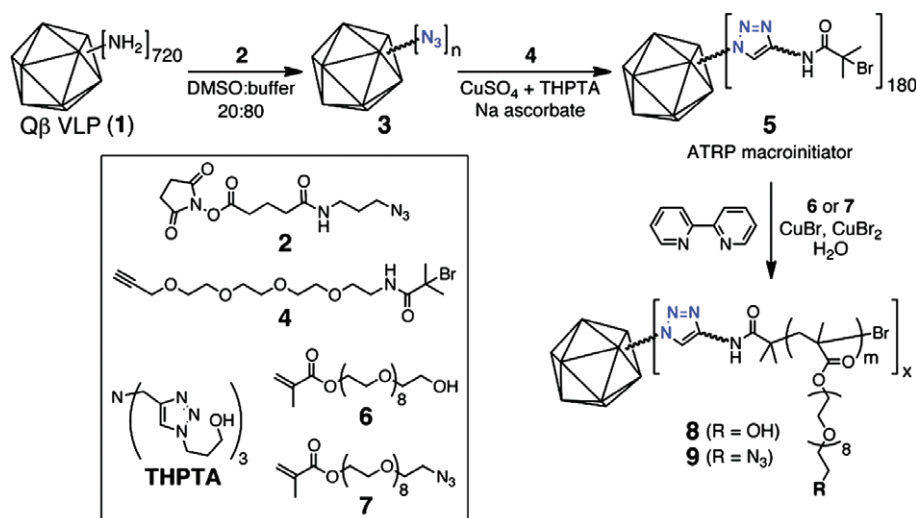
**FIGURE 4 |** (a) Schematic presentation of the attachment of poly(2-oxazoline) onto azide-functionalized Q $\beta$  exterior. PBS represents phosphate-buffered saline. (b) Molecular composition of poly(2-oxazoline) derivatives possessing various amounts of alkyne attachment points. (Reprinted with permission from Ref 28. Copyright 2011 John Wiley and Sons)

3 and 4). Polymerization catalyzed by a 2,2'-bipyridine/CuBr/CuBr<sub>2</sub> system was carried out in an air-free aqueous solution. The polymers that were obtained through ATRP also yielded a substitutable tertiary bromide at the terminus, thus allowing further modification with functional molecules. The azide-ended analog provided an extensible scaffold with abundant

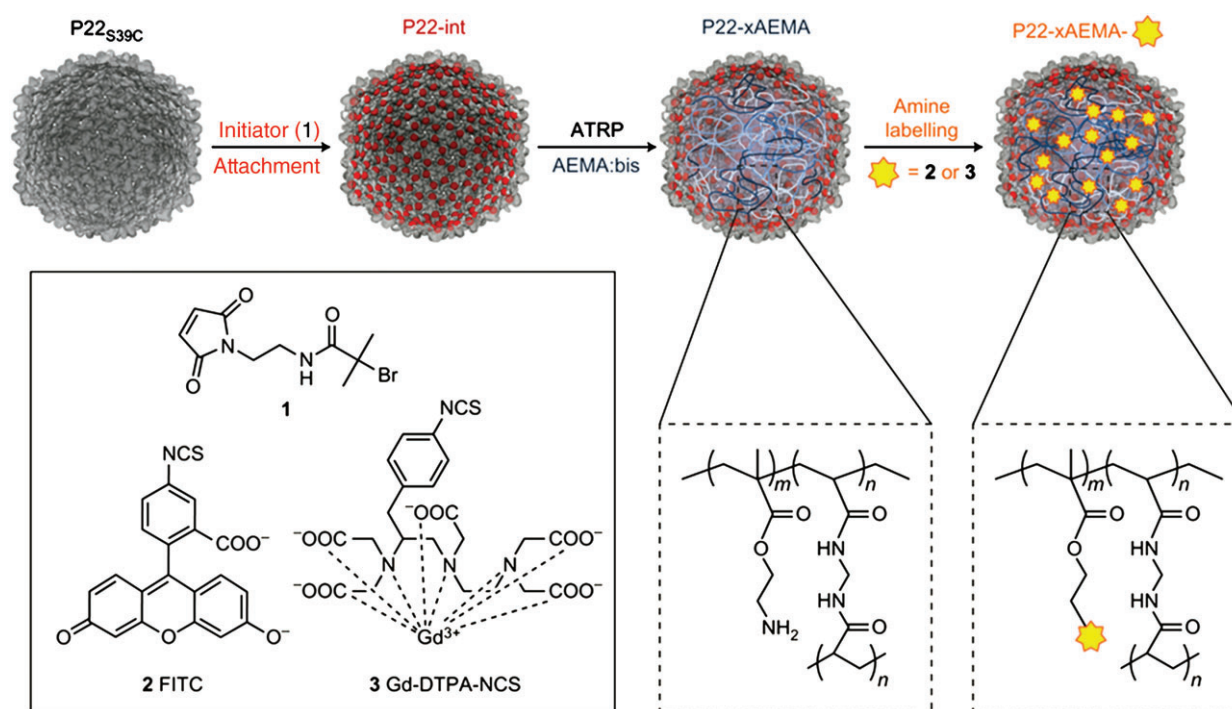
reactive sites for dense functionalization of Alexa Fluor 488 dye, gadolinium complex, and doxorubicin hydrazine, all of which were coupled with high efficiency (see below for the application of this system in drug delivery section of this review).

The installation of polymers of any appreciable size within the confined interior of a virus capsid can





**FIGURE 5** | Scheme of ATRP of poly(OEGMA) on outer shell of Q $\beta$ . (Reprinted with permission from Ref 58. Copyright 2011 American Chemical Society)



**FIGURE 6** | Scheme of internal initiator-attachment followed by ATRP of pAEMA and crosslinked with bisacrylamide (bis). The final step demonstrated the appended amine groups functionalized with FITC and Gd complex. (Reprinted with permission from Ref 57. Copyright 2012 Nature Publishing Group)

only be accomplished via a ‘graft from’ approach, since loading large polymers through the small apertures of VLPs is much less favorable than loading small initiators and small monomer species. This is predicated, importantly, on the interior being free from genome or scaffold proteins to provide

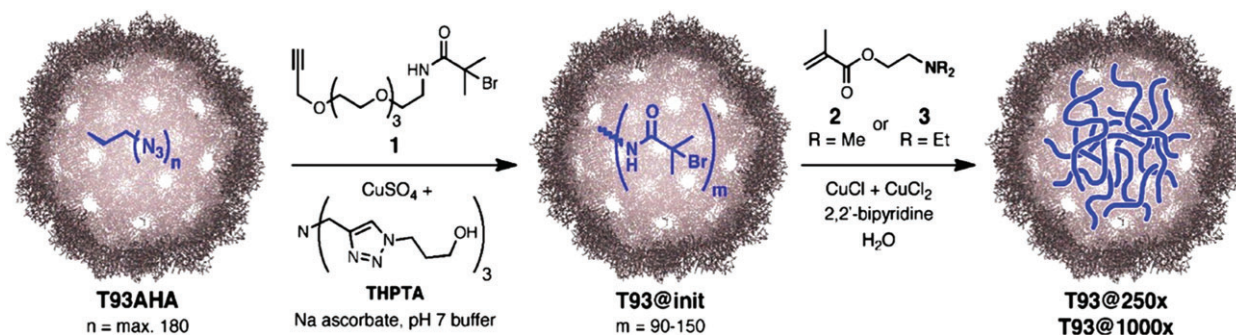
accessible reactive groups for initiator installation as well as space for polymer growth. Lucon et al.<sup>57</sup> performed Cu(I)/bipyridine catalyzed ATRP of 2-aminoethyl methacrylate (AEMA) within the expanded-form of a bacteriophage P22<sub>S39C</sub> mutant. The ethoxy maleimide initiator was conjugated to the

accessible thiol group within the VLP (Figure 6) and AEMA was allowed to diffuse into the virus in the presence of catalyst to produce an incarcerated polymer within the void space of the capsid. The confinement of polymerization within virus capsid was confirmed via TEM and DLS, both showing an unchanged diameter of the VLP after polymer growth; however, the as-obtained polymers showed relatively broad molecular weight distribution characterized by denaturing gel analysis indicating inhomogeneous polymerization. Nevertheless, the abundant amine groups on the side chains of AEMA demonstrated excellent modifiability, as indicated by migration of fluorescein-labeled polymer-protein composites in sodium dodecyl sulfate polyacrylamide gel electrophoresis (SDS PAGE) as well as a net shift of electrophoretic mobility between labeled and unlabeled subunits in native agarose gel electrophoresis. These experiments illustrate quite elegantly that this synthetic strategy possesses great potential in encapsulation of high-density functional molecules. A similarly elegant study from Hovlid et al.<sup>27</sup> extended interior polymerization by ATRP to a T93M Q $\beta$  mutant featuring 180 azide groups on the inner surface. As expected, the virus particle still needed to be emptied of random cellular RNA. Q $\beta$  cannot be disassembled reversibly to directly dump the RNA, so the group created a strategy to hydrolyze the RNA *in situ* in the presence of lead(II) acetate. As shown in Figure 7, following RNA hydrolysis and CuAAC attachment of the triglyme bromide initiator, 2-(dimethylaminoethyl methacrylate) (DMAEMA) was polymerized onto  $120 \pm 30$  of the approximately 150 initiators. Curiously, the as-prepared pDMAEMA@T93 Q $\beta$  did not show significantly improved thermal stability, presumably due to noncrosslinking of the polymers (*vide infra*). TEM characterization revealed no appreciable difference between macroinitiator and the polymer-virus composite, whereas

expanded hydrodynamic radii of the polymer-virus composites were found on both DLS and size exclusion chromatography (SEC). This led the group to conduct additional experiments to examine the confinement of the polymer within the capsid. The results revealed nondifferentiable binding affinity of anti-Q $\beta$  antibody to both the surfaces of the nonpolymerized virus particle as well as the polymerized virus particle. They further demonstrated that avidin could not access polymer-bound biotin within the virus. These data provided solid evidence that the virus capsid had effectively confined the growth and the configuration of the polymer inside.

### Physical Properties of Virus-Polymer Hybrids

Virus-polymer hybrid materials have shown advanced properties that arise from inheriting the unique nature of each component—virus and polymer—and the covalent chemistry that allows controllable and stable integration of functional molecules. In general, there are a few principle features of these as-prepared virus-polymer hybrids that have demonstrated great potential in material fabrication and bio-nanotechnology. Indeed, researchers have found that by integrating VLPs with polymers they can induce significant changes in their physical properties. For instance, in the aforementioned study by Manzenrieder et al.<sup>28</sup>, in which the outer shell of Q $\beta$  was conjugated with poly(2-oxazoline)s, all of the conjugated virus particles possessed enhanced thermal stability in their secondary structure, some were stable above 100°C. In contrast, significant differences were observed in the stability of tertiary and quaternary structures when the single-point attachment strategy was contrasted to the multi-point attachment strategy, which created ‘crosslinked’ virus particles (Figure 4). When subject to the high



**FIGURE 7** | Scheme of ATRP of pDMAEMA within T93 Q $\beta$  interior. (Reprinted with permission from Ref 27. Copyright 2014 American Chemical Society)

temperature region between 90 and 100°C, TEM characterization clearly demonstrated that the cross-linked VLPs remained intact whereas particles featuring single-point attachments had become irregular in shape, indicating disassembly of the spherical structure. This study does a good job illustrating that polymerization plays an important role in enhancing thermal stability of virus particles, especially for secondary protein structures, while higher order protein structural stability is further enhanced by adopting a crosslinking strategy.

Another interesting study done by Holder et al.<sup>52</sup> demonstrated that PEGylation of the exterior surface of TMV rendered amphiphilic solubility to the conjugates, as well as enhanced stability at temperatures upwards of 160°C! The TMV capsid was conjugated with 2kD PEGs in a 50% yield, giving about 1000 PEG chains per virus. The PEGylated TMV was stable in buffer solution and could be precipitated if the system were converted to a higher ionic strength. The precipitated PEGylated TMV then could be transferred into chloroform simply via solvent exchange. The researchers reported that these hybrids are stable in chloroform for a period up to 5 years! The stability of the TMV rods was investigated by measurement of particle size via DLS and observation of preserved rod-shape particle with appropriate size under TEM. The stability of PEGylated TMV was examined after they were heated above 100°C with no apparent change to the virus' morphology. They then showed PEGylated TMV could withstand temperatures as high as 160°C in benzyl alcohol. Moreover, the researchers found that PEGylated TMV hybrids could be stable under styrene polymerization conditions. The virus hybrids incorporated in the polystyrene were found to be stable after the temperature was elevated above the glass-transition temperature of the polystyrene. These results demonstrate a convincing case that PEGylation offers promise to bring TMV to the field of device fabrication.

Another feature that virus-polymer hybrids possess are controllable bio-interactions. A benefit to using VLPs over soft polymer and heterogeneous platforms is that the locations of reactive residues are known to atomic precision, allowing defined spatial organization of substituents on the surface. For instance, Astronomo et al. reported<sup>60</sup> a study attempting to mimic the glycan shield on the surface envelope spike of HIV using VLPs. The researchers' objective was to use Q $\beta$  and CCMV to mimic the conserved region of glycans typically found on HIV for recognition by the neutralizing antibody 2G12. The question was what effect, if any, would the

spatial organization or surface density have on 2G12 recognition? Q $\beta$  possesses four putatively functionalizable surface-exposed amines (three lysines and the N-terminus) per coat protein monomer. The researchers found that this provided a very densely packed array of surface attached glycans that might mimic the glycans found on HIV. Two noteworthy results were obtained: firstly, high surface density was required to bind 2G12 and only when Q $\beta$  was highly functionalized did this binding occur. Secondly, it was not possible to functionalize all four amines. The group found that converting the most surface-exposed lysine (K16) to a methionine did not decrease the number of surface-exposed glycans significantly. They reasoned that steric encumbrance between wild type functional groups prevented the simultaneous functionalization of lysine residues K12 and K16. This reaction inhibition by sterics is also suggestive of the conformational inflexibility of the surface-exposed amines, which are located 0.8 nm apart.

### Biodistribution of Virus-Polymer hybrids

PEG has been covalently attached to the surface of biomacromolecules, peptides and proteins, to improve their pharmacokinetic and pharmacodynamics properties. It has been known for some time that the PEGylation can help shield antigenic epitopes, which reduce reticuloendothelial (RES) clearance, passivate immune response, and biospecific interactions. VLPs exhibit promising potential to be used as drug delivery vehicles or imaging agent carriers toward cell and tissues; however, their tendency toward immunogenicity makes it necessary to hide their proteinaceous surfaces. An excellent early study on the use of PEG to afford immune passivation was done by Steinmetz et al.<sup>49</sup> who successfully PEGylated the surface of CPMV, and demonstrated their capacity to 'stealth' the VLP from immune recognition with a series of fundamental *in vitro* and *ex vivo* studies. PEG succinimidyl esters with a molecular weight between 1000 and 2000 Da were conjugated on the solvent-exposed lysine residues on CPMV. The attachment was confirmed by denaturing gel electrophoresis and the resulting particles were shown to remain intact post modification by native gel electrophoresis, DLS, SEC, and TEM.

Interestingly, even though PEG 2000 is a longer chain, DLS measurements show that the CPMV-PEG 2000 conjugate (P2) has a slightly smaller radius than the CPMV-PEG 1000 conjugate (P1). This implies that the PEG 2000 forms a more compact conformation on the CPMV surface than PEG 1000.

The group then used previously derived calculations<sup>61</sup> to determine that both the 1000 and 2000 Da PEG take a mushroom like conformation on the surface of CPMV rather than a brush conformation. Interestingly, even in this conformation, the total grafting areas of both P1 and P2 are incredibly small—below 1%. P2, for instance, has a grafting area—that is, the area covered by PEG—of only 0.83% of the total surface while P1, is less, at only 0.53%. Even so, *in vitro* and *ex vivo* analysis showed, PEGylated CPMV has a formulation dependent stealth effect that reduces interactions between viral particles and mammalian tumor cells and tumor tissues, with shielding efficiency of P2 at 80–90% compared to 30–55% of P1. Importantly, this study contributes to the cellular detection threshold of PEGylation on the surface of CPMV, which is required for efficient shielding. Compared to previously reported CPMV conjugates featuring PEG 3400,<sup>62</sup> PEG 5000,<sup>63</sup> and PEG 500<sup>55</sup> the conjugation of PEG 2000 seems to be optimized to not only consume the least amount of lysine attachment sites (<30), which leaves more surface for post functionalization, but also results in an effective shielding of the key areas involved in CPMV–cell interaction.

Another notable study on PEG as a means of altering the biophysical properties of a virus was done recently by the Steinmetz group.<sup>64</sup> The researchers modified the surface of Potato Virus X (PVX), a filamentous plant virus, using PEG and attempted to optimize pharmacokinetic profiles of the virus-PEG conjugate.<sup>65</sup> Pharmacokinetic results indicated PEG coatings induced a two-phase plasma clearance pattern combining renal filtration—the only mode for clearance with unmodified PVX—with mononuclear phagocyte system (MPS) clearance. Whole mouse imaging by fluorescence molecular tomography (FMT) shows a 3-day clearance of the PVX-PEG particles, a point the authors stress is important as it is better than synthetic rigid hard materials such as carbon nanotube and gold that commonly accumulate in the lung and liver tissues and remain there for weeks or months. PEGylation on PVX also reduces the virus' immunogenic properties, including antibody recognition and uptake by immune cells, and very notably did not induce an inflammatory response.

Finally, the authors were able to tailor the pharmacokinetic properties of PVX-PEG particle by altering the molecular weight and chain conformation (linear thread-like vs. branched and tree-like PEG) of the PEG coating on PVX. For linear PEG, higher molecular weight resulted in a 'brush-like' conformation, which has a longer circulation time

and better stealth effect compared to lower molecular weight PEG. On the other hand, branched PEG exhibits a more densely packed surface, which provided a superior stealth effect compared to linear PEG. This method makes it flexible enough to satisfy different applications that require longer (e.g., Passive tumor targeting, etc.) or shorter (e.g., receptor-targeted contrast agents) circulation time.

## CHEMICAL MODIFICATION OF VIRAL ARCHITECTURES TO ATTACH IMAGING AGENTS

The unique properties of viruses, combined with the relative ease of genetic and chemical modification, provide ideal platforms for the design of sensing and imaging agents.<sup>66–69</sup> Several excellent reviews<sup>13,36,68</sup> have been written on inorganic and organometallic MR contrast agents coupled to VLPs, so we will narrow our focus on the use of synthetic organic fluorescent dyes, which offer a relatively low cost means of imaging vasculature and disease within a few millimeters under the skin. Luminescent materials such as quantum dots, carbon nanotubes, and noble metal nanoparticles suffer from bioaccumulation, poor biocompatibility, and low water solubility. Synthetically, it is difficult to make these nanoparticles of uniform size and below the 6 nm limit to allow renal clearance. Additionally, modification can be difficult, as these man-made nanoparticles lack accessible functional handles. On the other hand, viruses and VLPs have many unique advantages compared to synthetic nanoparticles including monodispersity, high cell permeability, high aqueous solubility, and—as we have mentioned—they can be modified synthetically to attach multiple different ligands for targeting or to alter their chemical and biological stability.

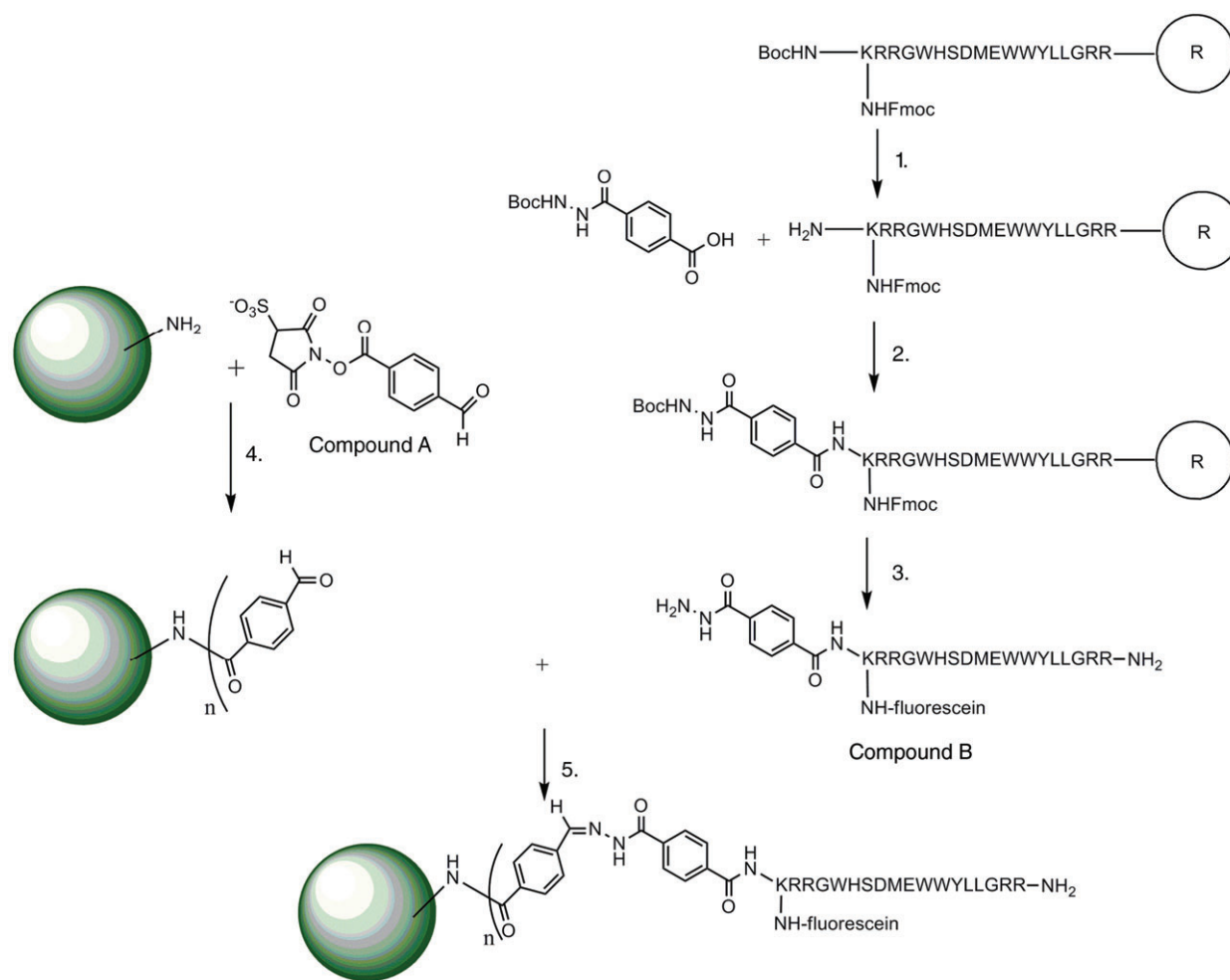
Conveniently, most coupled dyes can be commercially sourced as the N-hydroxysuccinimidyl (NHS) ester or isothiocyanate functionalized dye and attachment to the VLP is as easy as mixing the two together. It is also possible, and not all that much more challenging, to add a free alkyne handle for CuAAC chemistry on the VLP using one of the aforementioned strategies. The emergence of CuAAC chemistry has enabled a more modular approach to the attachment of fluorophores. Alkynyl or azide groups are easily installed on both the dyes as well as the VLPs and the subsequent CuAAC reaction typically proceeds quickly in dilute aqueous solution with very high yields. This is particularly important, as commercially obtained dyes are not cheap. A third method, discussed below, is conjugation by

formation of arylhydrazone, which is also a good choice to attach chromophores to VLPs.

Fluorescent dye labeling has proven to be a popular method for modification of VLPs for *in vivo* imaging. The multivalency of the VLPs in many cases allows for over one hundred copies of a single dye to be localized on the surface creating a very bright nanoparticle that can be easily traced as it moves through vasculature. An early example of coupling fluorescent dyes to VLPs was reported by the Manchester group, using Oregon Green-488 carboxylic acid to study the biodistribution of CPMV in mouse tissues *ex vivo*.<sup>70</sup> CPMV was chosen in this study because of its stability at low pH, high temperatures (up to 60°C), and in organic solvents such as DMSO. Actual *in vivo* imaging of dye conjugated VLPs in fluorescence whole animal imaging would not find use until the following year, when Lewis et al.<sup>62</sup> produced fluorescent CPMV by a similar synthetic

method. Alexa Fluor 555, Alexa Fluor 488 and fluorescein dyes containing NHS-esters were bound to CPMV. This bright nanoparticle provided visualization of the vasculature and blood flow to a depth of up to 500 μm in living mouse and chicken embryos. The particles were sufficiently bright that the researchers were able to visualize angiogenesis and human tumor vasculature.

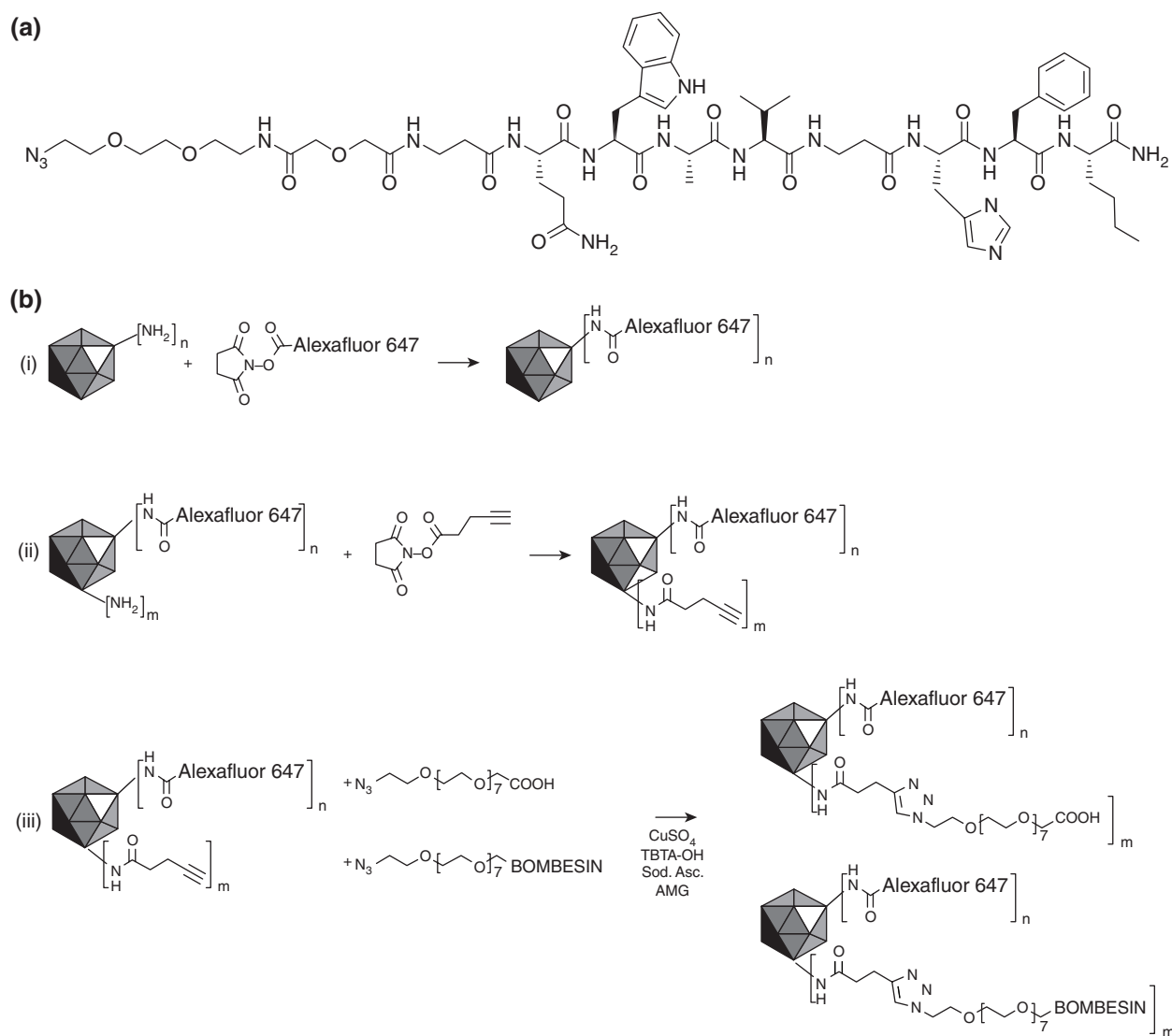
Diagnosing and imaging of disease is also a highly sought after goal of contrast agent development and, as in the case of targeted drug delivery, it is possible to append targeting elements to the exterior surface of VLPs side-by-side with the fluorophores. Dawson's group<sup>71</sup> modified CPMV with tunable densities of targeting ligand and a fluorescent PEGylated peptide using an efficient hydrazone ligation reaction (Figure 8). Briefly, CPMV was modified using a water-soluble 4-formylbenzoylsulfo-NHS ester to introduce benzaldehyde groups to surface



**FIGURE 8** | Synthesis of Fluorescein-F56 complex and conjugation to CPMV. (Reprinted with permission from Ref 71. Copyright 2010 American Chemical Society)

lysine residues. This reaction was very effective with about 280 of the 300 available amino reaction sites being modified. For subsequent conjugations, ligands containing an arylhydrazide group were appended to the benzaldehyde moieties on CPMV in weakly acidic buffer (pH = 5.5). For this work, two ligands were created: a fluorescein conjugated to a VEGFR-1-specific F56 peptide—a targeting ligand—or a fluorescein conjugated to a PEG group for improved plasma circulation time. These complexes were then attached to CPMV. The net result was a combination of 133 copies of Fluorescein-F56 complex and 55 copies of Fluorescein-PEG complex attached to one CPMV for a total of 188 fluorescent dyes per VLP. CPMV labeled with Fluorescein-F56 complex

and Fluorescein-PEG complex were found to efficiently target human endothelial cells that express high levels of VEGFR-1 but did not bind to fibroblasts cells, which lack VEGFR-1 expression. A potential drawback to this strategy, however, is partial ligand shielding by neighboring PEG chains. In a subsequent paper by Steinmetz et al.<sup>72</sup> the fluorescent dye was labeled directly on CPMV first, followed by a PEGylated targeting ligand. As depicted in Figure 9, NHS activated esters and CuAAC chemistry were used to modify CPMV particles with PEG, NIR dye, and the PEGylated targeting ligand bombesin. Bombesin is a 14 amino acid peptide that targets cell surface GRP (gastrin releasing peptide) receptors, which are aberrantly expressed in a number of



**FIGURE 9** | (a) Chemical structure of the bombesin analog covalently bound with a PEG linker. (b) Synthetic processes of Dye-labeled CPMV-PEG and CPMV-PEG-bombesin. (Reprinted with permission from Ref 72. Copyright 2011 John Wiley and Sons)

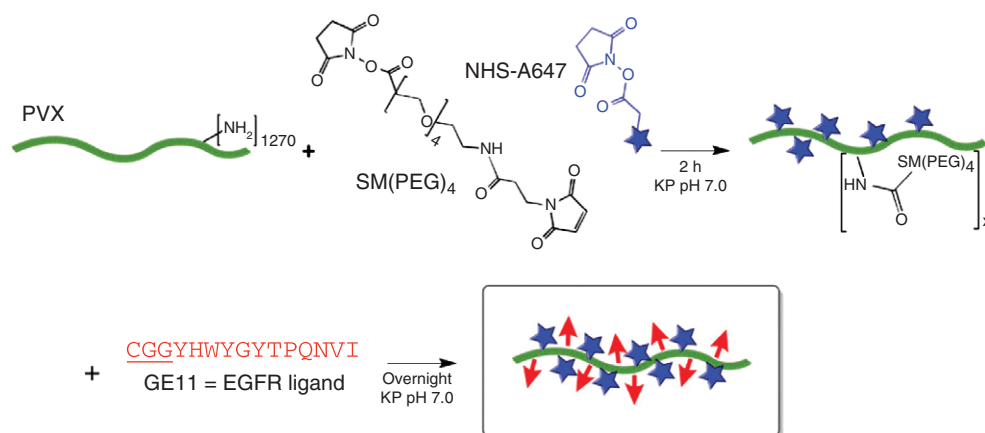
human cancers. To illustrate their targeting strategy, human PC-3 prostate cancer cells that over-expresses GRP receptors were used in cell uptake experiments. CPMV-PEG-bombesin demonstrated both specific targeting and significant uptake with this cell line. To further confirm that CPMV-PEG-bombesin could be used in intravital imaging of tumors, human PC-3 prostate cancer cells were xenografted onto the chorioallantoic membrane in chicken models. The authors reported that tumor homing using the CPMV-PEG-bombesin was achieved even when the tumor was only 5 mm in diameter.

Potato virus X (PVX)<sup>73</sup> and M13 bacteriophage<sup>74</sup> are highly anisotropic rod-shaped nanoparticles featuring large surface areas and thus an abundance of active reaction sites for modification. Additionally, recent data<sup>75,76</sup> has suggested rod-shaped materials may offer better disease targeting and pharmacokinetic properties compared to spherical materials. PVX is quite large at 515 nm × 13 nm, and is assembled from 1270 identical coat proteins, each of which provides a solvent-exposed lysine residue. In a recent publication from the Steinmetz group<sup>73</sup>, fluorescently labeled PVX coupled to GE11—a 12 peptide strand that targets epidermal growth factor receptor (EGFR)—was obtained by a two-step reaction, as illustrated in Figure 10. Firstly, lysines on PVX were covalently modified with both Alexa Fluor 647 and a maleimide-terminated PEG linker (SM(PEG)<sub>4</sub>). The maleimide-terminated linker was subsequently conjugated from the thiol group of the cysteine-terminated GE11 peptide. Cell targeting and imaging was then carried out utilizing four kinds of cancer cell lines and fluorescently labeled PVX-GE11 was found to selectively target EGFR<sup>+</sup> cell lines with no observable non-specific uptake in EGFR<sup>-</sup> cell lines.

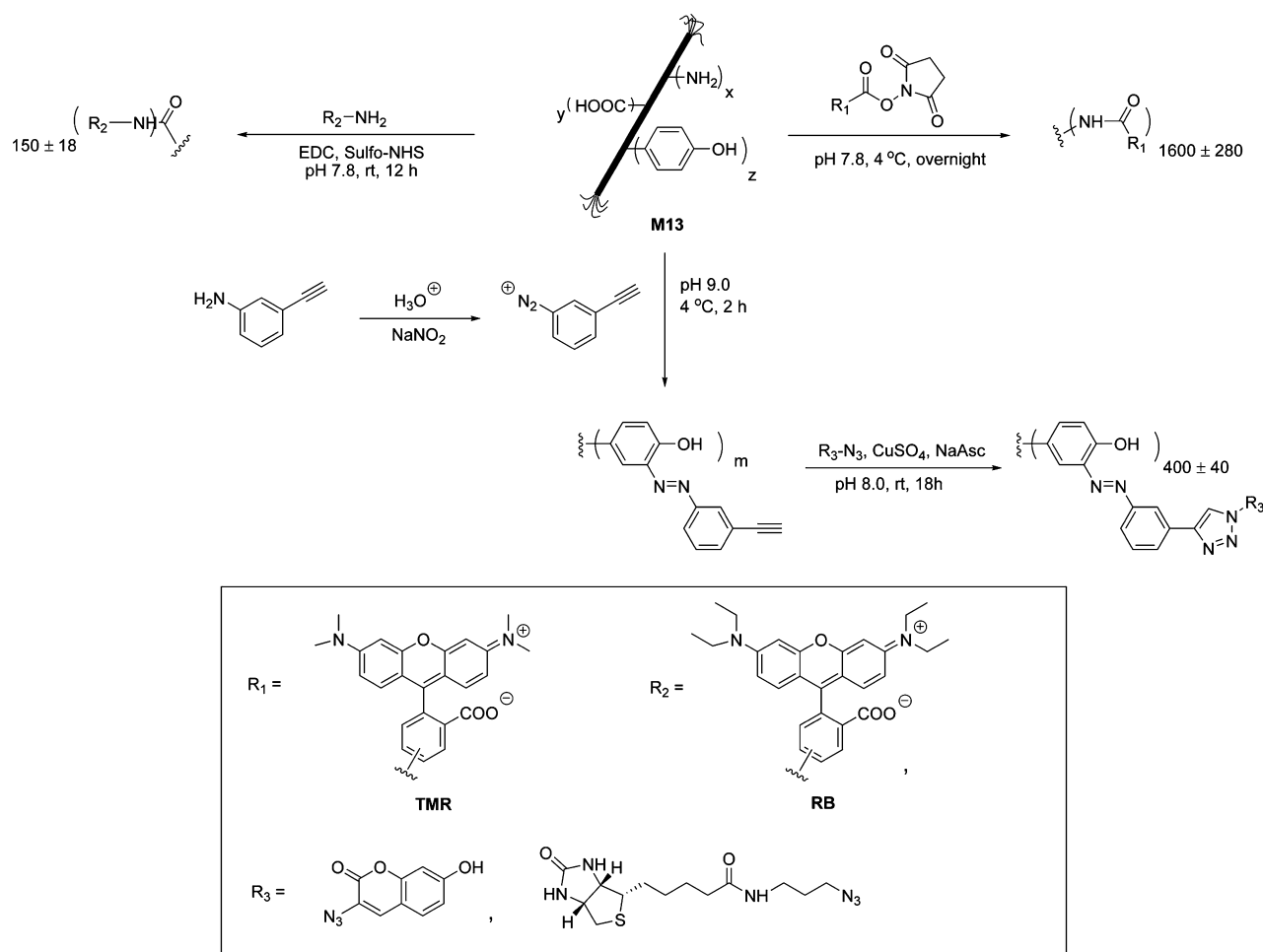
M13 is also a rod-shape virus with the size of 880 nm × 6.6 nm. Its capsid is composed of 2700 copies of the major coat protein P8 and the ends are capped with five copies of four kinds of minor coat proteins (P9, P7, P6, and P3). In total, there are three kinds of reactive groups on the M13 surface that can be chemically modified: the amino groups of lysine or the N-terminus, carboxylic acid groups of aspartic acid or glutamic acid, and the phenol groups of tyrosine. Bioconjugation<sup>74</sup> of these groups with small fluorescent molecules was demonstrated to compare the reactivity of each group (Figure 11). Amino-NHS coupling was used to modify both the lysine and the N-terminus. The result showed the N-terminus was more active than lysine reportedly because of its lower pKa. CuAAC chemistry was found to be another easy way to modify the M13 virus with small molecules. By modification of the tyrosine residue with a novel alkyne-functionalized diazonium reagent, dual-modified M13 particles conjugated with fluorescent dyes and cancer cell targeting folic acid motifs was synthesized and showed very good binding affinity to human KB cancer cells.

## CHEMICAL MODIFICATION OF VIRAL ARCHITECTURES FOR DRUG DELIVERY

The properties and chemistry we have discussed thus far about VLPs should illustrate why they would make an attractive target for drug delivery vehicles. They are naturally robust capsids evolutionarily directed to deliver delicate cargo to the interior of hostile territory. The topics we have covered clearly paint a picture that it is not only possible but also quite



**FIGURE 10** | Modification of PVX with PEG linker (SM(PEG)<sub>4</sub>), Alexa Fluor 647 NHS ester and subsequent labeled by GE11 peptide. (Reprinted with permission from Ref 73. Copyright 2015 American Chemical Society)



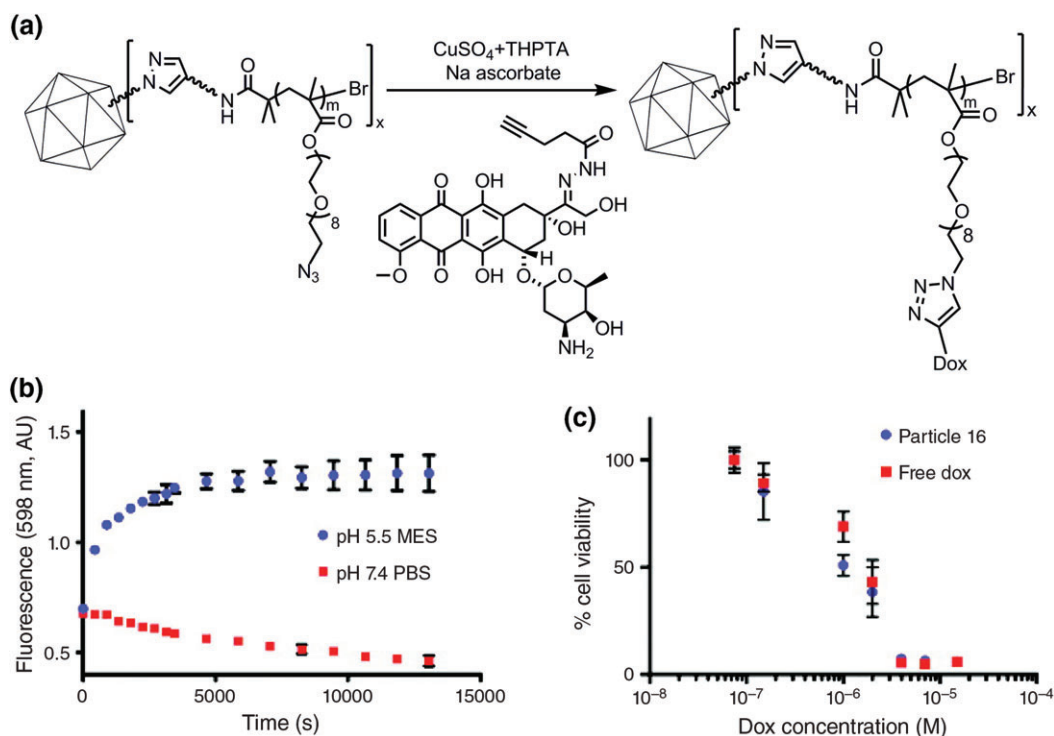
**FIGURE 11** | Different chemical modification approaches of M13 virus and structures of small molecules that were covalently bonding to M13. (Reprinted with permission from Ref 74. Copyright 2010 American Chemical Society)

straightforward to functionalize the exterior with, for instance, cell targeting ligands while covalently attaching drugs to the interior where they are hidden and safe from off target activation. While immunogenicity is a problem in some aspects, a topic expertly covered<sup>77</sup> in a recent review, it can also be an advantage. For instance, VLPs have been used as vaccine conjugates owing to their highly ordered structure and multivalent surface. Antigens have been immobilized on the surface of VLPs' coat proteins, and upon exposure to a patient's immune system, strong antibody responses against those antigens have been reported in both mice<sup>78</sup> and human subjects.<sup>79</sup> A noteworthy example from the Bachmann group used Q $\beta$  to create<sup>80</sup> a vaccine against nicotine. Nicotine derivative (O-succinyl-3'-hydroxymethyl-( $\pm$ )-nicotine) was linked to the surface-exposed lysine residues on bacteriophage Q $\beta$  such that each viral particle contained about 585 nicotine molecules. Since the driving

force of tobacco addiction is the result of nicotine's reinforcing effects within the brain, the aim here was to create a vaccine that would induce antibodies that bind nicotine in the blood, which would prevent nicotine from ever crossing the brain–blood barrier. In preclinical animal studies, they were able to demonstrate that the VLP based vaccine induces strong and specific IgG antibody responses against nicotine. They found that the uptake of nicotine by the brain could be reduced 61% compared to control in mice. In phase I studies, this vaccine was found to be safe and an anti-nicotine response was observed in 100% of subjects following a single injection. The subsequent phase II randomized trials suggested that this 'Nicotine-Q $\beta$  vaccine' has the potential to significantly increase continuous abstinence rates in smokers who were ready to quit.

While not a true 'drug delivery' system, the vaccine example illustrated above illustrates an





**FIGURE 12** | (a) Azido-functionalized polymer hybrid Q $\beta$  particle coupled with Doxorubicin with hydrazone linker via CuAAC reaction. (b) in vivo Doxorubicin release profile from Q $\beta$ -polymer conjugate at pH 5.5 and 7.4; (c) MTT assay for HeLa cell viability with particle conjugates and free Doxorubicin alone. (Reprinted with permission from Ref 58. Copyright 2011 American Chemical Society)

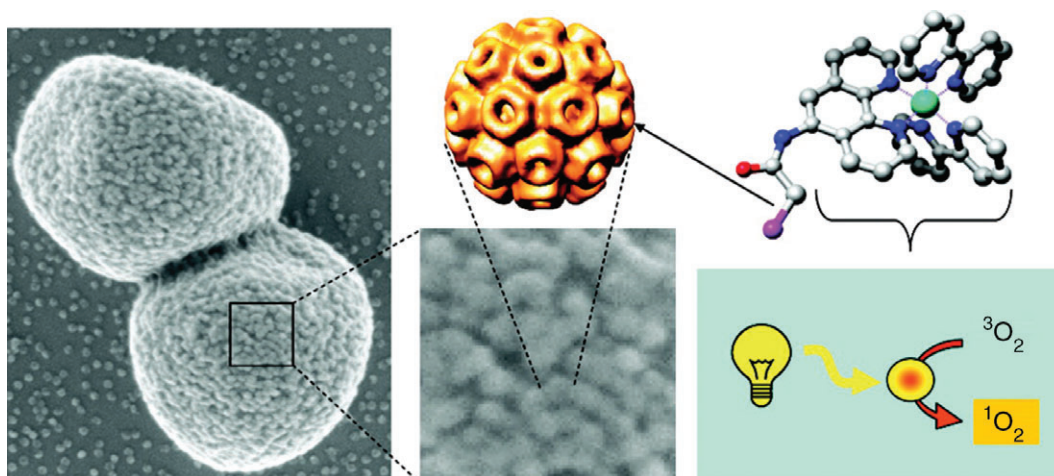
important point: attaching a drug to the surface of a viral particle for delivery may have the unintended consequence of eliciting antibodies against that drug—likely *not* the outcome desired in a true drug delivery application. Of course, inhibiting or hampering the immune system's access to the virus surface would undoubtedly mitigate any immune response. Coupled to the fact that minor immunological responses are found in many drug compounds with large hydrodynamic radii with little detriment to the patient, it stands to reason that continued and rigorous evaluation of VLPs as drug delivery agents should be pursued. Previously studied synthetic drug delivery vehicles, such as liposomes,<sup>81,82</sup> have poor stability and targeting performance and the controlled release of drugs from them has been difficult to realize. One possible solution to overcome this problem is to introduce a pH-sensitive spacer between a VLP delivery vehicle and target drug.<sup>83</sup> Hydrazone linkers are excellent for drug release systems, as they are stable in neutral pH, but can be rapidly hydrolyzed under acidic conditions. This hydrolysis can be triggered upon entry in the acidic environment of endosomal and lysosomal compartments (pH 4.5–5.5) of a cell. Based on this drug delivery strategy, the Finn group utilized<sup>58</sup> their

aforementioned Q $\beta$ -poly(OEGMA-N<sub>3</sub>) and attached Doxorubicin hydrazine with a terminal alkyne spacer under CuAAC conditions as shown in Figure 12(a). The resulting particles remained intact, had a narrow size distribution, and featured an average of 150 Dox molecules per particle as determined by spectrophotometry. The pH sensitivity of this Q $\beta$ -Dox conjugate was examined by fluorescence spectroscopy. Depicted in Figure 12(b), when the conjugate was incubated at pH 5.5, the maximum fluorescence intensity was observed after approximately 2 h, which supports the idea that Dox is released under acidic conditions, most likely through hydrazone bond cleavage. However, at pH 7.4, there was no observed fluorescence increase. This pH-sensitive virus-drug conjugate was also examined in HeLa cells by incubating in pH 7 buffer for 8 h followed by MTT assay. The conjugate demonstrated similar cytotoxicity to HeLa cells when compared to free Dox (Figure 12(c)). These results indicate that particles have been internalized and subsequently release the drug molecules in the acidic compartments within the cell leading to cell death.

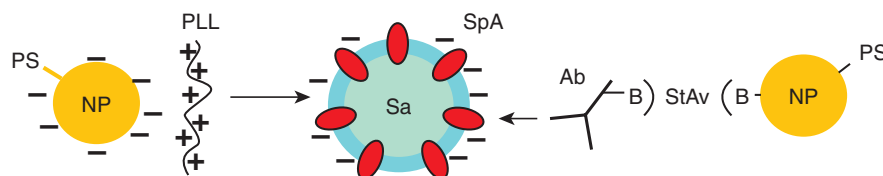
In addition, VLPs have been combined with photosensitizers for photodynamic therapy (PDT). PDT, also called photodynamic therapy, is based on the use of a photosensitizer (PS), which generates

reactive oxygen species (ROS) when excited by light at its resonant wavelength. ROS can access and destroy cell components, which leads to cell death. This technique has been used to kill cancer cells as well as bacteria; however, some challenges and concerns still remain in its application to human and microbes, such as collateral damage to healthy host tissue and lack of specific targeting. VLPs have a relatively large surface area for covalent modification and the multivalent surfaces featuring a defined ‘inside’ and ‘outside’ make VLPs ideally suited delivery vehicles for modification with PS on the inside and targeting ligands on the outside. The combination of genetic and chemical engineering strategies on VLPs provide more possibilities for multifunctional nanoplatforms that can selectively attach PS or ligands. Several VLP based photosensitizers have been studied. The groups of Douglas and Young<sup>84</sup> attached the functionalized photosensitizer Ru(bpy)<sub>2</sub>phen-IA to the cystines of genetically modified CCMV at surface accessible sites, as shown in

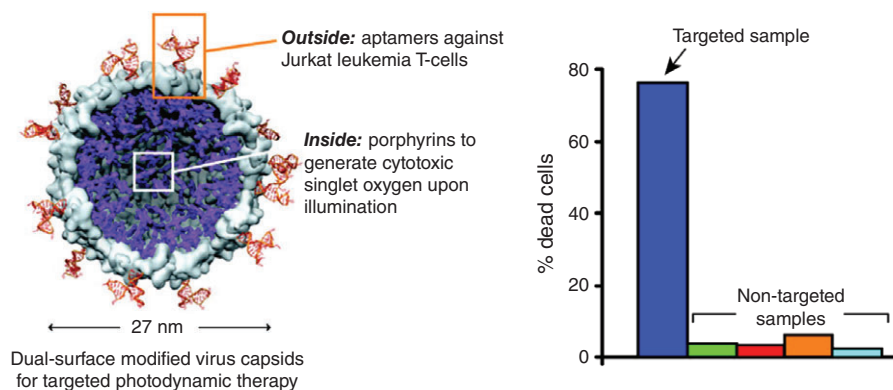
Figure 13. They constructed two systems that can target CCMV-PS conjugates to microbial pathogens—one using electrostatic interactions and another using complementary biological interactions. Electrostatic targeting of CCMV-PS to the negatively charged cell wall of *S. aureus*, a cationic polymer, poly-L-lysine (PLL) was used. PLL targeted CCMV-PS was able to obtain a higher local PS concentration, which enhanced its antibacterial effects upon light activation when compared to the nontargeted PLL free CCMV-PS. The group also biotinylated CCMV with sulfosuccinimidyl-6'-(biotinamido)-6-hexanamido hexanoate, which can selectively target protein A (SpA) in the cell wall of *S. aureus* cells using a streptavidin (StAv) linker (Figure 14). One site of StAv binds to biotinlayted CCMV-PS, while the other site binds to a biotinlyted anti-SpA monoclonal antibody (anti-SpAmAb-B), which can bind to the cell. The targeting delivery was significantly enhanced by complementary biotin–streptavidin interactions, compared to the unbiotinlyted control or free PS. While



**FIGURE 13** | The combination of CCMV and photosensitizer for PDT. (Left) FESEM image of CCMV-PS-biotin conjugate covering on the cell wall through complementary biological interaction; (upper middle) CCMV; (lower middle) zoomed in micrograph of targeted cell wall; (upper right) photosensitizer (Ru(bpy)<sub>2</sub>phen-IA); (lower right) cartoon represents the ROS generation upon illumination on the CCMV-PS conjugate. (Reprinted with permission from Ref 84. Copyright 2007 American Chemical Society)



**FIGURE 14** | (a) Targeting strategies using electrostatic (left) or biological interaction (right). PS: photosensitizer; NP: nanoparticle; PLL: poly-L-lysine; Sa: *S. aureus* cell; SpA: protein A; Ab: anti-SpA-mAb-B; B: bitotin; StAv: streptavidin. (Reprinted with permission from Ref 84. Copyright 2007 American Chemical Society)



**FIGURE 15** | Dual-surface modified bacteriophage MS2 capsid with photosensitizer and targeting ligands for photodynamic therapy, which significantly and specifically killed target cells. (Reprinted with permission from Ref 10. Copyright 2010 American Chemical Society)

the targeting with antibody conjugated PS was similar to the VLP-hybrid, the targeted CCMV nanoplat-form demonstrated a more uniform attachment to the bacterial cell surface.

Another example of photosensitization using VLPs was reported by the Francis group.<sup>10</sup> They orthogonally modified the inner and outer surfaces of bacteriophage mutant MS2. The photosensitizer porphyrin maleimide was attached to Cys87 (N87C) on the interior surface through a thiol-maleimide coupling reaction (Figure 15). This freed up the exterior surface to allow a cell-receptor-specific DNA aptamer that can specifically target cancer cells to be coupled through a NaIO<sub>4</sub>-mediated oxidative coupling reaction to an unnatural amino acid *p*-aminophenylalanine (*paF*.) Up to 180 porphyrin molecules, which can produce cytotoxic singlet oxygen under light irradiation, were connected to the cysteine residues, while approximately 20 copies of aptamer were covalently attached to the exterior surface of MS2. This viral vehicle specifically targeted Jurkat cells and selectively killed a significant amount of these cells in a 20-minute period upon illumination.

## CONCLUSION

Chemical modification of viruses to create hybrid materials has rapidly expanded. These stable protein structures permit a wider range of reactions than typical of proteinaceous biomolecules. Their unique topology—ordinarily impossible to access with such monodispersity—has created a niche in chemical virology that has no clear parallel in any other single chemical discipline. While this review could not address all the accomplishments presented in the field, it attempts to highlight some of the possibilities available with viral architectures. The high yield of virus production from plants and bacteria allow for gram scale reactions, depending on the virus, using biochemical methods that are very accessible. It is fair to say that a laboratory with no experience doing biochemical transformations could begin their first experiments on their own isolated virus within two months. As such, it is highly likely that the growing interest in the field will continue to contribute to interesting and important discoveries as new reactions and reaction methodologies emerge to allow new protein-synthetic hybrids.

## REFERENCES

- Nam KT, Kim D-W, Yoo PJ, Chiang C-Y, Meethong N, Hammond PT, Chiang Y-M, Belcher AM. Virus-enabled synthesis and assembly of nanowires for lithium ion battery electrodes. *Science* 2006, 312:885–888.
- Chen X, Gerasopoulos K, Guo J, Brown A, Wang C, Ghodssi R, Culver JN. Virus-enabled silicon anode for lithium-ion batteries. *ACS Nano* 2010, 4:5366–5372.
- Pomerantseva E, Gerasopoulos K, Chen X, Rubloff G, Ghodssi R. Electrochemical performance of the nanostructured biotemplated V2O5 cathode for lithium-ion batteries. *J Power Sources* 2012, 206:282–287.
- Nam KT, Wartena R, Yoo PJ, Liau FW, Lee YJ, Chiang Y-M, Hammond PT, Belcher AM. Stamped microbattery electrodes based on self-assembled M13 viruses. *Proc Natl Acad Sci USA* 2008, 105:17227–17231.

- Royston E, Ghosh A, Kofinas P, Harris MT, Culver JN. Self-assembly of virus-structured high surface area nanomaterials and their application as battery electrodes. *Langmuir* 2008, 24:906–912.
- Scolaro LM, Castriciano MA, Romeo A, Micali N, Angelini N, Lo Passo C, Felici F. Supramolecular binding of cationic porphyrins on a filamentous bacteriophage template: toward a noncovalent antenna system. *J Am Chem Soc* 2006, 128:7446–7447.
- Miller RA, Presley AD, Francis MB. Self-assembling light-harvesting systems from synthetically modified tobacco mosaic virus coat proteins. *J Am Chem Soc* 2007, 129:3104–3109.
- Nam YS, Shin T, Park H, Magyar AP, Choi K, Fantner G, Nelson KA, Belcher AM. Virus-templated assembly of porphyrins into light-harvesting nanoantennae. *J Am Chem Soc* 2010, 132:1462–1463.
- Niu Z, Bruckman MA, Li S, Lee LA, Lee B, Pingali SV, Thiyagarajan P, Wang Q. Assembly of tobacco mosaic virus into fibrous and macroscopic bundled arrays mediated by surface aniline polymerization. *Langmuir* 2007, 23:6719–6724.
- Stephanopoulos N, Tong GJ, Hsiao SC, Francis MB. Dual-surface modified virus capsids for targeted delivery of photodynamic agents to cancer cells. *ACS Nano* 2010, 4:6014–6020.
- Carette N, Engelkamp H, Akpa E, Pierre SJ, Cameron NR, Christianen PCM, Maan JC, Thies JC, Weberskirch R, Rowan AE, et al. A virus-based biocatalyst. *Nat Nanotechnol* 2007, 2:226–229.
- Patterson DP, Schwarz B, Waters RS, Gedeon T, Douglas T. Encapsulation of an enzyme cascade within the bacteriophage P22 virus-like particle. *ACS Chem Biol* 2014, 9:359–365.
- Steinmetz NF. Viral nanoparticles as platforms for next-generation therapeutics and imaging devices. *WIREs Nanomed Nanobiotechnol* 2010, 6:634–641.
- Dragnea B, Chen C, Kwak E-S, Stein B, Kao CC. Gold nanoparticles as spectroscopic enhancers for in vitro studies on single viruses. *J Am Chem Soc* 2003, 125:6374–6375.
- Qazi S, Liepold LO, Abedin MJ, Johnson B, Prevelige P, Frank JA, Douglas T. P22 viral capsids as nanocomposite high-relaxivity MRI contrast agents. *Mol Pharm* 2013, 10:11–17.
- Stevens TK, Palaniappan KK, Ramirez RM, Francis MB, Wemmer DE, Pines A. Hypercast detection of a 129Xe-based contrast agent composed of cryptophane-a molecular cages on a bacteriophage scaffold. *Magn Reson Med* 2012, 69:1245–1252.
- Brasch M, Voets IK, Koay MST, Cornelissen JJLM. Phototriggered cargo release from virus-like assemblies. *Faraday Discuss* 2013, 166:47–57.
- Tong GJ, Hsiao SC, Carrico ZM, Francis MB. Viral capsid DNA aptamer conjugates as multivalent cell-targeting vehicles. *J Am Chem Soc* 2009, 131:11174–11178.
- Steinmetz NF. Viral nanoparticles in drug delivery and imaging. *Mol Pharm* 2013, 10:1–2.
- Ohtake N, Niikura K, Suzuki T, Nagakawa K, Mikuni S, Matsuo Y, Kinjo M, Sawa H, Ijiro K. Low pH-triggered model drug molecule release from virus-like particles. *ChemBioChem* 2010, 11:959–962.
- West KR, Otto S. Reversible covalent chemistry in drug delivery. *Curr Drug Discov Technol* 2005, 2:123–160.
- Ma Y, Nolte RJM, Cornelissen JJLM. Virus-based nanocarriers for drug delivery. *Adv Drug Deliver Rev* 2012, 64:811–825.
- Sitasuwan P, Lee LA, Li K, Nguyen HG, Wang Q. Rgd-conjugated rod-like viral nanoparticles on 2d scaffold improve bone differentiation of mesenchymal stem cells. *Front Chem* 2014, 2:31.
- Zan X, Feng S, Balizan E, Lin Y, Wang Q. Facile method for large scale alignment of one dimensional nanoparticles and control over myoblast orientation and differentiation. *ACS Nano* 2013, 7:8385–8396.
- Fowler CE, Shenton W, Stubbs G, Mann S. Tobacco mosaic virus liquid crystals as templates for the interior design of silica mesophases and nanoparticles. *Adv Mater* 2001, 13:1266–1269.
- Radloff C, Vaia RA, Brunton J, Bouwer GT, Ward VK. Metal nanoshell assembly on a virus bioscaffold. *Nano Lett* 2005, 5:1187–1191.
- Hovlid ML, Lau JL, Breitenkamp K, Higginson CJ, Laufer B, Manchester M, Finn MG. Encapsidated atom-transfer radical polymerization in Q $\beta$  virus-like nanoparticles. *ACS Nano* 2014, 8:8003–8014.
- Manzenrieder F, Luxenhofer R, Retzlaff M, Jordan R, Finn MG. Stabilization of virus-like particles with poly(2-oxazoline)s. *Angew Chem Int Ed* 2011, 50:2601–2605.
- Speir JA, Munshi S, Wang G, Baker TS, Johnson JE. Structures of the native and swollen forms of cowpea chlorotic mottle virus determined by X-ray crystallography and cryo-electron microscopy. *Structure* 1995, 3:63–78.
- Wei N, Heaton LA, Morris TJ, Harrison SC. Structure and assembly of turnip crinkle virus: Vi. Identification of coat protein binding sites on the RNA. *J Mol Biol* 1990, 214:85–95.
- Butler PJG. Self-assembly of tobacco mosaic virus: the role of an intermediate aggregate in generating both specificity and speed. *Phil Trans R Soc Lond* 1999, 354:537–550.
- Wang Q, Lin T, Tang L, Johnson JE, Finn MG. Icosahedral virus particles as addressable nanoscale building blocks. *Angew Chem Int Ed* 2002, 41:459–462.
- Lammers T, Kiessling F, Hennink WE, Storm G. Drug targeting to tumors: principles, pitfalls and

- (pre-) clinical progress. *J Control Release* 2012, 161:175–187.
34. Soo Choi H, Liu W, Misra P, Tanaka E, Zimmer JP, Itty Ipe B, Bawendi MG, Frangioni JV. Renal clearance of quantum dots. *Nat Biotechnol* 2007, 25:1165–1170.
  35. Prasuhn DE, Singh P, Strable E, Brown S, Manchester M, Finn MG. Plasma clearance of bacteriophage Q $\beta$  particles as a function of surface charge. *J Am Chem Soc* 2008, 130:1328–1334.
  36. Schwarz B, Douglas T. Development of virus-like particles for diagnostic and prophylactic biomedical applications. *WIREs Nanomed Nanobiotechnol* 2015, 7:722–735.
  37. Stephanopoulos N, Francis MB. Choosing an effective protein bioconjugation strategy. *Nat Chem Biol* 2011, 7:876–884.
  38. Debets MF, van Berkel SS, Dommerholt J, Dirks AJ, Rutjes FPJT, van Delft FL. Bioconjugation with strained alkenes and alkynes. *Acc Chem Res* 2011, 44:805–815.
  39. Sunasee R, Narain R. Covalent and noncovalent bioconjugation strategies. In: *Chemistry of Bioconjugates*. Hoboken, NJ: John Wiley & Sons, Inc; 2014, 1–75. doi: 10.1002/9781118775882.ch1.
  40. Francis MB, Bernard JML. Chemical strategies for the covalent modification of filamentous phage. *Front Microbiol* 2014, 5:734.
  41. Chung W-J, Lee D-Y, Yoo SY. Chemical modulation of M13 bacteriophage and its functional opportunities for nanomedicine. *Int J Nanomedicine* 2014, 9:5825–5836.
  42. Bundy BC, Swartz JR. Efficient disulfide bond formation in virus-like particles. *J Biotechnol* 2011, 154:230–239.
  43. Golmohammadi R, Fridborg K, Bundule M, Valegård K, Liljas L. The crystal structure of bacteriophage Q $\beta$  at 3.5 Å resolution. *Structure* 1996, 4:543–554.
  44. Pauly H. Über Die Konstitution Des Histidins. I. Mitteilung. *Hoppe-Seyler's Z Physiol Chem* 1904, 42:508–518.
  45. Pauly H. Zur Kenntnis Der Diazoreaktion Des Eiweißes. *Hoppe-Seyler's Z Physiol Chem* 1915, 94:284–290.
  46. Hooker JM, Kovacs EW, Francis MB. Interior surface modification of bacteriophage Ms2. *J Am Chem Soc* 2004, 126:3718–3719.
  47. Schlick TL, Ding Z, Kovacs EW, Francis MB. Dual-surface modification of the tobacco mosaic virus. *J Am Chem Soc* 2005, 127:3718–3723.
  48. Kovacs EW, Hooker JM, Romanini DW, Holder PG, Berry KE, Francis MB. Dual-surface-modified bacteriophage Ms2 as an ideal scaffold for a viral capsid-based drug delivery system. *Bioconjug Chem* 2007, 18:1140–1147.
  49. Steinmetz NF, Manchester M. Pegylated viral nanoparticles for biomedicine: the impact of peg chain length on Vnp cell interactions in vitro and ex vivo. *Biomacromolecules* 2009, 10:784–792.
  50. Fisher KD, Stallwood Y, Green NK, Ulbrich K, Mautner V, Seymour LW. Polymer-coated adenovirus permits efficient retargeting and evades neutralising antibodies. *Gene Ther* 2001, 8:341–348.
  51. Green NK, Herbert CW, Hale SJ, Hale AB, Mautner V, Harkins R, Hermiston T, Ulbrich K, Fisher KD, Seymour LW. Extended plasma circulation time and decreased toxicity of polymer-coated adenovirus. *Gene Ther* 2004, 11:1256–1263.
  52. Holder PG, Finley DT, Stephanopoulos N, Walton R, Clark DS, Francis MB. Dramatic thermal stability of virus–polymer conjugates in hydrophobic solvents. *Langmuir* 2010, 26:17383–17388.
  53. Comellas-Aragonès M, de la Escosura A, Dirks AJ, van der Ham A, Fusté-Cuñé A, Cornelissen JJLM, Nolte RJM. Controlled integration of polymers into viral capsids. *Biomacromolecules* 2009, 10:3141–3147.
  54. Gupta SS, Raja KS, Kaltgrad E, Strable E, Finn MG. Virus-glycopolymer conjugates by copper(I) catalysis of atom transfer radical polymerization and azide-alkyne cycloaddition. *Chem Commun* 2005, 34:4315–4317.
  55. Raja KS, Wang Q, Gonzalez MJ, Manchester M, Johnson JE, Finn MG. Hybrid virus–polymer materials. 1. Synthesis and properties of peg-decorated cowpea mosaic virus. *Biomacromolecules* 2003, 4:472–476.
  56. Lucon J, Edwards E, Qazi S, Uchida M, Douglas T. Atom transfer radical polymerization on the interior of the P22 capsid and incorporation of photocatalytic monomer crosslinks. *Eur Polym J* 2013, 49:2976–2985.
  57. Lucon J, Qazi S, Uchida M, Bedwell GJ, LaFrance B, Prevelige PE, Douglas T. Use of the interior cavity of the P22 capsid for site-specific initiation of atom-transfer radical polymerization with high-density cargo loading. *Nat Chem* 2012, 4:781–788.
  58. Pokorski JK, Breitenkamp K, Liepold LO, Qazi S, Finn MG. Functional virus-based polymer–protein nanoparticles by atom transfer radical polymerization. *J Am Chem Soc* 2011, 133:9242–9245.
  59. Hong V, Presolski SI, Ma C, Finn MG. Analysis and optimization of copper-catalyzed azide–alkyne cycloaddition for bioconjugation. *Angew Chem Int Ed* 2009, 48:9879–9883.
  60. Astronomo RD, Kaltgrad E, Udit AK, Wang S-K, Doores KJ, Huang C-Y, Pantophlet R, Paulson JC, Wong C-H, Finn MG, et al. Defining criteria for oligomannose immunogens for hiv using icosahedral virus capsid scaffolds. *Chem Biol* 2010, 17:357–370.
  61. de Gennes PG. Polymers at an interface; a simplified view. *Adv Colloid Interface Sci* 1987, 27:189–209.

62. Lewis JD, Destito G, Zijlstra A, Gonzalez MJ, Quigley JP, Manchester M, Stuhlmann H. Viral nanoparticles as tools for intravital vascular imaging. *Nat Med* 2006, 12:354–360.
63. Destito G, Yeh R, Rae CS, Finn MG, Manchester M. Folic acid-mediated targeting of cowpea mosaic virus particles to tumor cells. *Chem Biol* 2007, 14:1152–1162.
64. Shukla S, Ablack AL, Wen AM, Lee KL, Lewis JD, Steinmetz NF. Increased tumor homing and tissue penetration of the filamentous plant viral nanoparticle potato virus X. *Mol Pharm* 2013, 10:33–42.
65. Lee KL, Shukla S, Wu M, Ayat NR, El Sanadi CE, Wen AM, Edelbrock JF, Pokorski JK, Commandeur U, Dubyak GR, et al. Stealth filaments: polymer chain length and conformation affect the in vivo fate of pegylated potato virus X. *Acta Biomater* 2015, 19:166–179.
66. Li F, Wang Q. Fabrication of nanoarchitectures templated by virus-based nanoparticles: strategies and applications. *Small* 2014, 10:230–245.
67. Li K, Nguyen HG, Lu X, Wang Q. Viruses and their potential in bioimaging and biosensing applications. *Analyst* 2010, 135:21–27.
68. Bruckman MA, Yu X, Steinmetz NF. Engineering Gd-loaded nanoparticles to enhance mri sensitivity via T1 shortening. *Nanotechnology* 2013, 24:462001–462021.
69. Michael AB, Xin Y, Nicole FS. Engineering Gd-loaded nanoparticles to enhance Mri sensitivity via T1 shortening. *Nanotechnology* 2013, 24:462001.
70. Rae CS, Wei Khor I, Wang Q, Destito G, Gonzalez MJ, Singh P, Thomas DM, Estrada MN, Powell E, Finn MG, et al. Systemic trafficking of plant virus nanoparticles in mice via the oral route. *Virology* 2005, 343:224–235.
71. Brunel FM, Lewis JD, Destito G, Steinmetz NF, Manchester M, Stuhlmann H, Dawson PE. Hydrazone ligation strategy to assemble multifunctional viral nanoparticles for cell imaging and tumor targeting. *Nano Lett* 2010, 10:1093–1097.
72. Steinmetz NF, Ablack AL, Hickey JL, Ablack J, Manocha B, Mymryk JS, Luyt LG, Lewis JD. Intravital imaging of human prostate cancer using viral nanoparticles targeted to gastrin-releasing peptide receptors. *Small* 2011, 7:1664–1672.
73. Chariou PL, Lee KL, Wen AM, Gulati NM, Stewart PL, Steinmetz NF. Detection and imaging of aggressive cancer cells using an epidermal growth factor receptor (Egfr)-Targeted filamentous plant virus-based nanoparticle. *Bioconjug Chem* 2015, 26:262–269.
74. Li K, Chen Y, Li S, Nguyen HG, Niu Z, You S, Mello CM, Lu X, Wang Q. Chemical modification of M13 bacteriophage and its application in cancer cell imaging. *Bioconjug Chem* 2010, 21:1369–1377.
75. Decuzzi P, Godin B, Tanaka T, Lee SY, Chiappini C, Liu X, Ferrari M. Size and shape effects in the biodistribution of intravascularly injected particles. *J Control Release* 2010, 141:320–327.
76. Geng Y, Dalhaimer P, Cai S, Tsai R, Tewari M, Minko T, Discher DE. Shape effects of filaments versus spherical particles in flow and drug delivery. *Nat Nanotechnol* 2007, 2:249–255.
77. Jennings GT, Bachmann MF. Immunodrugs: therapeutic Vlp-based vaccines for chronic diseases. *Annu Rev Pharmacol Toxicol* 2009, 49:303–326.
78. Jegerlehner A, Tissot A, Lechner F, Sebbel P, Erdmann I, Kündig T, Bächli T, Storni T, Jennings G, Pumpens P, et al. A molecular assembly system that renders antigens of choice highly repetitive for induction of protective B cell responses. *Vaccine* 2002, 20:3104–3112.
79. Ambühl PM, Tissot AC, Fulurija A, Maurer P, Nussberger J, Sabat R, Nief V, Schellekens C, Sladko K, Roubicek K, et al. A vaccine for hypertension based on virus-like particles: preclinical efficacy and phase I safety and immunogenicity. *J Hypertens* 2007, 25:63–72.
80. Maurer P, Jennings GT, Willers J, Rohner F, Lindman Y, Roubicek K, Renner WA, Müller P, Bachmann MF. A therapeutic vaccine for nicotine dependence: preclinical efficacy, and phase I safety and immunogenicity. *Eur J Immunol* 2005, 35:2031–2040.
81. Tachibana R, Harashima H, Shono M, Azumano M, Niwa M, Futaki S, Kiwada H. Intracellular regulation of macromolecules using Ph-sensitive liposomes and nuclear localization signal: qualitative and quantitative evaluation of intracellular trafficking. *Biochem Biophys Res Commun* 1998, 251:538–544.
82. Gullotti E, Yeo Y. Extracellularly activated nanocarriers: a new paradigm of tumor targeted drug delivery. *Mol Pharm* 2009, 6:1041–1051.
83. Ulbrich K, Etrych T, Chytil P, Pechar M, Jelinekova M, Rihova B. Polymeric anticancer drugs with Ph-controlled activation. *Int J Pharm* 2004, 277:63–72.
84. Suci PA, Varpness Z, Gillitzer E, Douglas T, Young M. Targeting and photodynamic killing of a microbial pathogen using protein cage architectures functionalized with a photosensitizer. *Langmuir* 2007, 23:12280–12286.
85. Hooker JM, O'Neil JP, Romanini DW, Taylor SE, Francis M. Genome-free viral capsids as carriers for positron emission tomography radiolabels. *Mol Imaging Biol* 2008, 10:182–191.
86. Datta A, Hooker JM, Botta M, Francis MB, Aime S, Raymond KN. High relaxivity gadolinium hydroxypyridonate-viral capsid conjugates: nanosized Mri contrast agents 1. *J Am Chem Soc* 2008, 130:2546–2552.
87. Capehart SL, ElSohly AM, Obermeyer AC, Francis MB. Bioconjugation of gold nanoparticles through

- the oxidative coupling of ortho-aminophenols and anilines. *Bioconjug Chem* 2014, 25:1888–1892.
88. Capehart SL, Coyle MP, Glasgow JE, Francis MB. Controlled integration of gold nanoparticles and organic fluorophores using synthetically modified Ms2 viral capsids. *J Am Chem Soc* 2013, 135:3011–3016.
89. Obermeyer AC, Capehart SL, Jarman JB, Francis MB. Multivalent viral capsids with internal cargo for fibrin imaging. *PLoS One* 2014, 9:e100678.
90. Carrico ZM, Romanini DW, Mehl RA, Francis MB. Oxidative coupling of peptides to a virus capsid containing unnatural amino acids. *Chem Commun* 2008, 10:1205–1207.
91. Farkas ME, Aanei IL, Behrens CR, Tong GJ, Murphy ST, O'Neil JP, Francis MB. Pet imaging and biodistribution of chemically modified bacteriophage Ms2. *Mol Pharm* 2013, 10:69–76.
92. Stephanopoulos N, Carrico ZM, Francis MB. Nano-scale integration of sensitizing chromophores and porphyrins with bacteriophage Ms2. *Angew Chem Int Ed* 2009, 48:9498–9502.
93. El Muslemany KM, Twite AA, ElSohly AM, Obermeyer AC, Mathies RA, Francis MB. Photoactivated bioconjugation between Ortho-azidophenols and anilines: a facile approach to biomolecular photopatterning. *J Am Chem Soc* 2014, 136:12600–12606.
94. Garimella PD, Datta A, Romanini DW, Raymond KN, Francis MB. Multivalent, high-relaxivity Mri contrast agents using rigid cysteine-reactive gadolinium complexes. *J Am Chem Soc* 2011, 133:14704–14709.
95. Wu W, Hsiao SC, Carrico ZM, Francis MB. Genome-free viral capsids as multivalent carriers for taxol delivery. *Angew Chem Int Ed* 2009, 48:9493–9497.
96. Wu M, Shi J, Fan D, Zhou Q, Wang F, Niu Z, Huang Y. Biobehavior in normal and tumor-bearing mice of tobacco mosaic virus. *Biomacromolecules* 2013, 14:4032–4037.
97. Bruckman MA, Hern S, Jiang K, Flask CA, Yu X, Steinmetz NF. Tobacco mosaic virus rods and spheres as supramolecular high-relaxivity Mri contrast agents. *J Mater Chem B* 2013, 1:1482–1490.
98. Bruckman MA, Kaur G, Lee LA, Xie F, Sepulveda J, Breitenkamp R, Zhang X, Joralemon M, Russell TP, Emrick T, et al. Surface modification of tobacco mosaic virus with “click” chemistry. *ChemBioChem* 2008, 9:519–523.
99. Yin Z, Nguyen HG, Chowdhury S, Bentley P, Bruckman MA, Miermont A, Gildersleeve JC, Wang Q, Huang X. Tobacco mosaic virus as a new carrier for tumor associated carbohydrate antigens. *Bioconjug Chem* 2012, 23:1694–1703.
100. Hu J, Wang P, Zhao X, Lv L, Yang S, Song B, Wang Q. Charge-transfer interactions for the fabrication of multifunctional viral nanoparticles. *Chem Commun* 2014, 50:14125–14128.
101. Wang Q, PONGKWAN S, Lee LA, Li K, Nguyen HG. Rgd-Conjugated rod-like viral nanoparticles on 2d scaffold improved bone differentiation of mesenchymal stem cells. *Front Chem* 2014, 2:31.
102. Chen L, Zhao X, Lin Y, Huang Y, Wang Q. A supramolecular strategy to assemble multifunctional viral nanoparticles. *Chem Commun* 2013, 49:9678–9680.
103. Bruckman MA, Liu J, Koley G, Li Y, Benicewicz B, Niu Z, Wang Q. Tobacco mosaic virus based thin film sensor for detection of volatile organic compounds. *J Mater Chem* 2010, 20:5715–5719.
104. Bruckman MA, Jiang K, Simpson EJ, Randolph LN, Luyt LG, Yu X, Steinmetz NF. Dual-modal magnetic resonance and fluorescence imaging of atherosclerotic plaques in vivo using Vcam-1 targeted tobacco mosaic virus. *Nano Lett* 2014, 14:1551–1558.
105. Miller RA, Stephanopoulos N, McFarland JM, Rosko AS, Geissler PL, Francis MB. Impact of assembly state on the defect tolerance of TMV-based light harvesting arrays. *J Am Chem Soc* 2010, 132:6068–6074.
106. Obermeyer AC, Jarman JB, Francis MB. N-terminal modification of proteins with O-aminophenols. *J Am Chem Soc* 2014, 136:9572–9579.
107. Yin Z, Comellas-Aragones M, Chowdhury S, Bentley P, Kaczanowska K, BenMohamed L, Gildersleeve JC, Finn MG, Huang X. Boosting immunity to small tumor-associated carbohydrates with bacteriophage Q $\beta$  capsids. *ACS Chem Biol* 2013, 8:1253–1262.
108. Mead G, Hiley M, Ng T, Fihn C, Hong K, Groner M, Miner W, Drugan D, Hollingsworth W, Udit AK. Directed polyvalent display of sulfated ligands on virus nanoparticles elicits heparin-like anticoagulant activity. *Bioconjug Chem* 2014, 25:1444–1452.
109. Pokorski JK, Hovlid ML, Finn MG. Cell targeting with hybrid Q $\beta$  virus-like particles displaying epidermal growth factor. *ChemBioChem* 2011, 12:2441–2447.
110. Banerjee D, Liu AP, Voss NR, Schmid SL, Finn MG. Multivalent display and receptor-mediated endocytosis of transferrin on virus-like particles. *ChemBioChem* 2010, 11:1273–1279.
111. Steinmetz NF, Hong V, Spoerke ED, Lu P, Breitenkamp K, Finn MG, Manchester M. Buckyballs meet viral nanoparticles: candidates for biomedicine. *J Am Chem Soc* 2009, 131:17093–17095.
112. Kaltgrad E, O'Reilly MK, Liao L, Han S, Paulson JC, Finn MG. On-virus construction of polyvalent glycan ligands for cell-surface receptors. *J Am Chem Soc* 2008, 130:4578–4579.
113. Prasuhn JDE, Yeh RM, Obenaus A, Manchester M, Finn MG. Viral Mri contrast agents: coordination of Gd by native virions and attachment of Gd complexes by azide-alkyne cycloaddition. *Chem Commun* 2007, 12:1269–1271.